ACS Chemical Neuroscience
Cite This: ACS Chem. Neurosci. 2020, 11, 105−120
Review
pubs.acs.org/chemneuro

Molecular Dynamics Simulations Applied to Structural and Dynamical Transitions of the Huntingtin Protein: A Review

Sanda Nastasia Moldovean and Vasile Chiş*

Babeş-Bolyai University, Faculty of Physics, Kogălniceanu 1, RO-400084 Cluj-Napoca, Romania

ABSTRACT: Over the recent years, Huntington's disease (HD) has become widely discussed in the scientific literature especially because at the mutant level there are several contradictions regarding the aggregation mechanism. The specific role of the physiological huntingtin protein remains unknown, due to the lack of characterization of its entire crystallographic structure, making the experimental and theoretical research even harder when taking into consideration its involvement in multiple biological functions and its high affinity for different interacting partners. Different types of models, containing fewer (not more than 35 Qs) polyglutamine residues for the WT structure and above 35 Qs for the mutants, were subjected to classical or advanced MD simulations to establish the proteins' structural stability by evaluating their conformational changes. Outside the polyQ tract, there are two other regions of interest (the N17 domain and the polyP rich domain) considered to be essential for the aggregation kinetics at the mutant level. The polymerization process is considered to be dependent on the polyQ length. As the polyQ tract's dimension increases, the structures present more β-sheet conformations. Contrarily, it is also considered that the aggregation stability is not necessarily dependent on the number of Qs, while the initial stage of the aggregation seed might play the decisive role. A general assumption regarding the polyP domain is that it might preserve the polyQ structures soluble by acting as an antagonist for β-sheet formation.

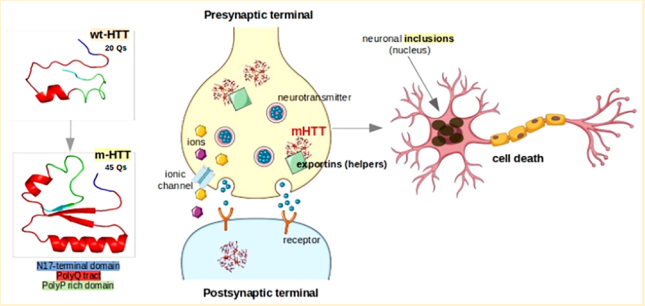

KEYWORDS: *Huntington's disease, molecular dynamics, trinucleotide repeats, mutant HTT, polyglutamine, neurodegeneration*

1. INTRODUCTION

Huntington's disease (HD) is an inherited condition characterized by multiple neurodegenerative dysfunctions that generate progressive disruptions in the brain cells, leading to abnormal motor coordination (also called *chorea*) as the earliest symptom. At the advanced stages of the disease, cognitive and psychiatric symptoms become severe enough to be recognized and assessed to a particular onset or extent, although the symptoms, especially the behavioral ones, can undoubtedly vary between patients.[1−4]

Huntingtin (HTT) protein is expressed in all cells, with a higher concentration in the brain;[5−7] it is mostly located in the cytoplasm, but it is also found in small amounts in the nucleus. It is considered to be essential for brain development, in terms of maintaining a proper communication between neurons.[8−14] However, the specific pathways involved at the level of this protein with respect to its function are still unknown.

Therefore, specific computational studies have been performed regarding involvement of mutation at the atomistic level, for a better understanding of its biological behavior. On the other hand, the wild-type HTT (wt-HTT) is a large, multidomain protein that can dynamically travel between different cellular compartments and can easily interact with over 100 other proteins, consequently being involved in multiple biological functions.[9,10,12,15−19] However, structural information on HTT protein at atomic resolution is not available.[20]

The experimental studies into this neurodegenerative disease also encounter significant limitations due to the deficient characterization of the crystallographic structure of the entire protein, especially because of the many interacting-partners involved; thus accurate conduct of the protein cannot be easily determined.[19,21]

The best characterized sequence of the entire (67 exons) wt-HTT is Exon 1 (Ex.1), with an N-terminal domain consisting of 17 amino acids, bound to the so-called polyQ stretch where mutation takes place, and followed by a polyP (polyproline) region, which is considered to act as a protein-interacting domain as well.[20,22−27]

The particular gene involved encoding HTT protein is IT-15′. IT-15′ stands for "interesting transcript 15′". At the level of this gene, in physiological conditions (wt-HTT), the section containing trinucleotide CAG repeats (polyQ stretch) is no longer than 35 repeats. In contrast, the cause of HD is considered to be an enlarged number (>35) of CAG repeats at the level of the first exon of the IT-15′ gene.[22] These numbers of the trinucleotide repeats are not well established, and

Received: October 17, 2019
Accepted: December 16, 2019
Published: December 16, 2019

DOI: 10.1021/acschemneuro.9b00561
ACS Chem. Neurosci. 2020, 11, 105−120

Table 1. Previously Published Papers Including MD Simulations on HTT Protein

ref	structure of interest and PDB files	simulation package and technique	force field, simulation time (ST), temperature (T), and other specifications	conclusions
Côté et al.[38]	dimeric (Q40 × 2) hexameric (Q40 × 6), and octameric (Q30 × 8) polyQ (Q_{40}) nanotubes at an all-atom level; comparison with similar structures built with Q30 was also made; sequence for HTT N-terminal domain: MATLEKLMKAFESLKSF (residues 1−17)	GROMACS NPT ensemble	OPLS-AA/L force field; additional structural stability checking with Gromos53a6 Amber99SB-ILDN Charmm27 force fields; T = 300 and 330 K; ST = 100, 200, and 250 ns	• nanotubes (formed of $polyQ_n$ tracts) were stable over the 100 ns simulations at 330 K for all of the used force fields; • they have proposed that their structural model might be considered as a building block to form longer nanotubes with higher structural stability; • HTT N-terminal domain clearly favors oligomerization process by increasing the stability of β-sheet-rich conformations; • for longer nanotubes, the stabilization is also made by HTT N-terminal domain, due to reduction of solvent accessibility of the glutamine residues
Kang et al.[40]	full Ex1-HTT on five different polyQ-lengths: Q22, Q36, Q40, Q46, and Q65	GROMACS; temperature replica exchange MD	OPLS-AA/L force field; ST = 500 ns/replica	• longer polyQ-lengths tend to adopt supercompact structures, due to the "glue-like" behavior of Q's side chains; • possible explanation for the insoluble behavior of the polyQ domains might be that the Q side chains tend be buried inside their inner core
Priya and Gromiha[45]	HTT-N terminal region with 17 Q residues (from PDB 3IO4) and 36 Q residues with the insertion of 3 histidine residues (from PDB 4FE8); Sequences: MATLEKLMKAFESLKSF$(Q)_n$ with n = 27, 34, 35, 36, 40, or 50 and MATLEKLMKAFESLKSF$(Q)_n$(P)11QLPQ(P)3QAQPLLPQ with n = 27 or 50	GROMACS; NPT ensemble	AMBER99SB-ILDN force field; T = 300 K; ST = 500 ns	• with the increased number of Q residues, the structures adopt different but more stable β-sheet conformations; critical length (the proposed threshold) for disease progression was predicted to be ≥40 Q residues; • N-terminal residues (N17) present different behavior in comparison to polyP tracts; • N17 deletion decreases the aggregation rate, while polyP tracts restrict it
Długosz and Trylska[52]	HTT-N17Q (WT-HTT) and HTT-N55Q (m-HTT) 1st sequence: MATLEKLMKAFESLKSFpolyQ(17)polyP(11)LPQPPPQAQPLLPQPQ 2nd sequence: MATLEKLMKAFESLKSFpolyQ(55)polyP(11)LPQPPP-QAQPLLPQPQ	AMBER 9[193] NAMD; replica exchange MD	FF03 force field;[194] Amber FF03; T = 290−377.1 K	• α-helical configurations were observed for both input sequences; • helical content decreases by increasing the temperature; • during the aggregation process, polyQ tracts expose the α-helical headpieces to solvent, by altering (disrupting) the hydrophobic interactions with the polyP tracts
Bevivino and Loll[57]	extended β-sheet of parallel/antiparallel strands of polyQ	CHARMM	mixed QMM mechanical force fields; ST not available	• parallel polyQ β-sheets may be energetically more favorable than antiparallel β-sheets.
Wang et al.[67]	N-acetyl-$(Gln)_5$-N-methylamide and N-acetyl-$(Gln)_{15}$-N-methylamide	GROMACS	OPLS-AA force field; 60 × 15 ns for Q5; 90 × 15 ns for Q15	• glutamine residues tend to adopt helical conformations
Stork et al.[68]	modeled input structures (poly-Gln β-helices) from PDB 1LXA	EGO-MMII[195] NPT ensemble	CHARMM22 force field; ST = 2−10 ns; T = 300 K	• dimers of 36 Q repeats are required for the initial aggregation seed of HTT
Merlino et al.[69]	several GLN β-helix models of different size (36-Gln, 41-Gln, 61-Gln, and 161-Gln)	GROMACS	CHARMM22 force field; T = 300 K; ST = 5 ns	• shorter helix models are unstable and present irregular structures, while the longer-helix models (>40 Gln) present dynamic regular structure (consistent with the disease threshold of ≈36 Gln repeats)
Ogawa et al.[70]	20Q, 25Q, 30Q, 37Q, and 40Q models of 18.5 residues/coil and 20 residues/coil	AMBER7	AMBER99 force field; T = 310 K; ST = 1 ns	• structure stability increases by increasing the number of Q repeats; • there is a critical Q number (30Q) above which the structure is kept stable (also proposed by Perutz et al.[56])
Rossetti et al.[71]	circular and triangular β-helix models consisting of 266 Qs (circular model) or 179 Qs (triangular model)	GROMACS	GROMOS96 T gradually increased from 0 to 300 K; ST = 20 ns	• "structural threshold" hypothesis was not supported; • in comparison to the circular model, the triangular model presented a larger number of Qs in random coil conformation;

DOI: 10.1021/acschemneuro.9b00561
ACS Chem. Neurosci. 2020, 11, 105−120

Table 1. continued

ref	structure of interest and PDB files	simulation package and technique	force field, simulation time (ST), temperature (T), and other specifications	conclusions
				• structural stability of the two models and their H-bond content were comparable
Marchut and Hall[77−79]	isolated large polyglutamine peptide (16, 24, 32, 36, 40, or 48 residues long) systems	discontinuous molecular dynamics (DMD)	PRIME* protein model based on extended polyQ representations	• stability of the polyQ aggregates increases by increasing the number of Q residues; • large β-sheets (tube-like annular structures) were observed for the system with 24 polyQ chains (16 residues long); • these findings are in good agreement with Perutz's model[56] (polyQ conformation being similar to "water-filled nanotubes")
Zanuy et al.[80]	$(D_2Q_{15}K_2)_m$ peptide, m = number of strands	CHARMM NVT ensemble	CHARMM 22 force field	• β-bend motifs imply connections between long parallel β-sheets and allow the growth of partially ordered fibril structures; • proposed model permits the peptide backbone to change direction with minimal loss of main chain hydrogen bonds
Lakhani et al.[87]	total of 12 models: monomeric XN1 with full flanking regions; variant without the polyP regions; isolated polyQ(n) peptide with n = 23, 36, 40, and 47 residues	replica exchange discrete MD	Medusa force field; ST = 50 ns/replica T = 500 K; continuous potential for each pair of two atoms was reduced to a series of square well potentials[87]	• Nt17 residues alone adopt random coil conformations regardless of the polyQ length; • For XN1Q36−47, Nt17 residues form β-sheet conformations more often than α-helical conformations; • with increased the polyQ length, the Nt17 residues prefer β-sheet conformations; • in the models without polyP, Nt17 presented more β-strands, with a higher preference for β-sheet conformations; these configurations are believed to affect the polyQ regions
Kelley et al.[99]	headpieces of the huntingtin protein (N17HTT)	GROMACS modified to include an simulated tempering algorithm[196]	AMBER force field; ST = 285−592 K	• HTT-N17 structure is an amphipathic one; • two helix bundle was correlated to the most populated state for N17HTT, although a significant percentage of the structures do still adopted a single linear helix; • fundamental role of HTT-N17 is to initialize the dimerization states and to drag polyQ tracts close to each other, in order to initialize their nucleation process
Nakano et al.[105]	monomeric polyQ peptides, Q9, Q11, Q13, Q15; pairs of polyQ monomers with different lengths, Q3, Q5, Q7, Q9; Q7 parallel and antiparallel dimers	Amber10 replica exchange MD and multiple MD	parm96 force field; T = 241−800 K/replica; ST = 30 ns MD run	• polyQ dimers form antiparallel β-sheet structures; • long monomeric polyQ chains act as an aggregation seed while forming pairs of antiparallel β-sheet structures within a single chain
Gómez-Sicilia et al.[112]	variety of Q_n structures (particularly Q_{20} and Q_{60}) presenting different secondary structure bias: no bias; preference to α-helix; preference to antiparallel β-strands; preference to parallel β-strands	GROMACS with PLUMED extension	AMBER99SB force field	• longer polyQ expansions present higher mechanical stability than the shorter ones and were seen to be more susceptible to form knotted structures; • knotted regions consist of an average of 35Q residues (similar to HD threshold); • mechanical stability was observed for peptides having more than 35Q residues
Laghaei and Mousseau[114]	polyQ monomers and dimers with chain lengths of 30, 40, and 50 residues	replica exchange MD	coarse-grained OPEP force field; T = 250−700 K; ST = 200 ns, 300 ns, and additional 100 ns	• monomers adopt configurations from α-helical to random coil structures, making them unable to start the aggregation process; • dimers (of Q = 40) form antiparallel β-sheets and triangular and circular β-helical conformations

DOI: 10.1021/acschemneuro.9b00561
ACS Chem. Neurosci. 2020, 11, 105−120

Table 1. continued

ref	structure of interest and PDB files	simulation package and technique	force field, simulation time (ST), temperature (T), and other specifications	conclusions
Miettinen et al.[115]	various conformations of polyQ peptide with 40 Q residues (considered to be the pathological range)	GROMACS (v.4.0.7 for GROMOS ff and v.4.5.3 for CHARMM ff)	united-atom GROMOS43a1 and the all-atom CHARMM27 force fields; T = 310 K; ST = 100 ns	• compared to the steric zipper or nanotube-like structures, α-helical and β-hairpin conformations (β-sheet and β-sheet stack) present higher stability, making them prone to form or initiate the polyQ fibrillar-like structures
Zhang et al.[117]	compact β variants for Ex1-HTT N-terminal domain: 42Q, PGQ9, EDQ9, PGQW, and PGQ6/12	NAMD NPT ensemble	CHARMM 22/27 force field; T = 300 K; ST = 10 and 20 ns	• PGQP monomer was the least stable of all the examined sequences. • even if Ex.1-HTT EDQ_9 was not seen to form aggregates in transfected cells (experimental part of the study), in MD simulations EDQ9 turned into highly compact β structure; • in contrast, PGQ6/12 presented loss in its β-sheet conformation; • constructs with expanded polyQ β-strands were stabilized due to their main-chain hydrogen bonding
Barton et al.[127]	chymotrypsin inhibitor 2 (CI2) chimeras containing Q_n inserts (between residues 43 and 44) with n = 4, 6, 8, 10, 20, 30, 35, 40, 50, 60, and 80, PDB 1CQ4; structures were modeled using a "beads-on-a-string" method	discrete MD, replica exchange DMD	T = 0.7−1.35 (for monomers) and 0.95−1.16 (for dimers) in units of $\epsilon/(k_BT)$, k_B being the Boltzmann constant	• monomer folding cooperativity decreases for polyQ-expanded structures (above the pathogenic threshold); this finding might represent a valuable insight into early stages of m-HTT aggregation process; • process of dimer formation is based on inter-Q H-bonding
Côté et al.[155]	HTT 17-amino-acid amino-terminal segment on a POPC (1-palmitoyl-2-oleoyl-*sn*-glycero-3-phosphocholine) bilayer, PDB 2LD2 + a single α-helix	GROMACS with PLUMED plug-in MD and Hamiltonian replica exchange (HREX) simulations, NPT ensemble	MBER99sb*-ILDN protein force field + the Berger phospholipid force field; ST = 250, 500, and 1000 ns	• HTT17 on a POPC membrane induces local mechanical perturbations of the bilayer, such as reducing phospholipid area by decreasing the membrane; • electrostatic interactions are clearly dependent on the phospholipid type, without being related to the HTT17 configuration; • with respect to the secondary structure configuration, the HTT17 monomers adopt stable α-helices on the POPC bilayer
Gopalakrishnan et al.[179]	HTT-Ex.1 (0Q, 17Q, and 36Q) with the SH3 domain of SH3GL3 interacting protein (PDB 2EW3)	GROMACS + HADDOCK software for docking HTT-Q_n with SH3GL3	GROMOS96 43a1 force field NPT ensemble; T = 300 K; ST - 10 ns without any restriction	• stronger interaction between HTT-36Q and SH3GL3, in comparison to HTT-17Q and the binding partner; • interaction of HTT protein with SH3GL3 is strongly correlated to the length of the polyQ tract
Vöpel et al.[182]	HTT-Q_{55}-Ex1 in the absence/presence of CLR01 tweezer	NAMD, replica exchange MD, classical MD, QM/MM	CHARMM27 force field	• results showed structural rearrangements within HTT-Q_{55}-Ex1, upon its binding to CLR01; this rearrangement was correlated with an inhibition of the HTT-Ex1 aggregation process • N17 was able to bind three CLR01 molecules simultaneously; • in the absence of CLR01, N17 shows high α-helical content, while the presence of the tweezer significantly decreases the α-helical conformation of N17

[a]The system presented no explicit water molecules; therefore, the hydrogen bonds between backbone or side-chain atoms and water molecules were not determined.

DOI: 10.1021/acschemneuro.9b00561
ACS Chem. Neurosci. 2020, 11, 105−120

therefore an exact starting point from which the mutation is being triggered remains elusive.

It has been demonstrated, however, that as a consequence to this quantitative mutation, an enlarged protein is being formed in brain cells leading to an accelerated neuropathological phenotype.[28−32] The biochemical studies and electron microscopy (EM) analysis revealed the presence of mutant HTT (m-HTT) at the neuronal level as forms of aggregated inclusions presenting a fibrillar morphology.[32−35]

The aim of this review is to summarize the existing data in the literature with a primarily interest in m-HTT structural characterization. Another purpose is to give an overview of molecular dynamics (MD) simulation results with respect to m-HTT's conformational changes and their involvement in disease threshold assessment.

2. MATERIALS AND METHODS

From a total number of 19976 articles found with a basic search using "Huntington's disease" tag, the addition of "molecular dynamics" restricted the number of the articles to 165. From the 165 articles, not all of the scientific papers were focused straight on HD in MD.

The particular keywords used for data collection were "huntingtin", "HD", "molecular dynamics", "MD", "HD dynamics", "trinucleotide repeats", "mutant HTT", "polyglutamine", "β-sheets", "protein aggregation" and "neurodegeneration". The main sources of data were PubMed, Science Direct, and Web of Science databases, although random searches on Google using different combinations of these keywords were also made. In addition to this, the references from the most suitable articles were also used to complete the final list of citations.

3. RESULTS AND DISCUSSION

3.1. Structural Characterization of Ex.1-HTT Protein.

The full-length of HTT has 3144 residues (348 kDa). Because of its large size, in order to understand the aggregation process at the mutant level, research studies[36−40] were mainly focused on the polyQ fragments and the formation of amyloid-like fibrils.[41] It has been demonstrated that the polyQ stretch is directly involved in this aggregation process, although this crucial stage of the disease has not been sufficiently clarified. Most of the recent published review articles were focused on HTT's biological mechanisms.[40,42−45] At this level, it is crucial to understand the mutants' structural transitions from monomers to aggregated fibrils and to consider that simple polyQ monomers might be intrinsically toxic. Without the biological and biochemical concepts within the protein, an adequate assessment of its behavior at an atomistic level is roughly impossible.

An optimal way to address HTT protein structural stability and its aggregation behavior would be to assess the conformational changes in different types of models. In Table 1, we summarize the previously published papers on the topic of this review, including the structures of interest, the used simulation package and technique, force fields, temperatures, and simulation times (where available), and the main conclusions of the papers.

All-atom MD simulations of the entire Ex.1-HTT protein were made over different polyglutamine lengths. It has been shown that the full-length HTT structure is overall conserved in time; nonetheless, at the level of polyglutamine tail, the secondary structure presents significant variations.

The secondary structure of the N-terminal domain (Figure 1) from the Ex.1-HTT was determined using X-ray crystallography.[22,46−48] The available PDB file formats used

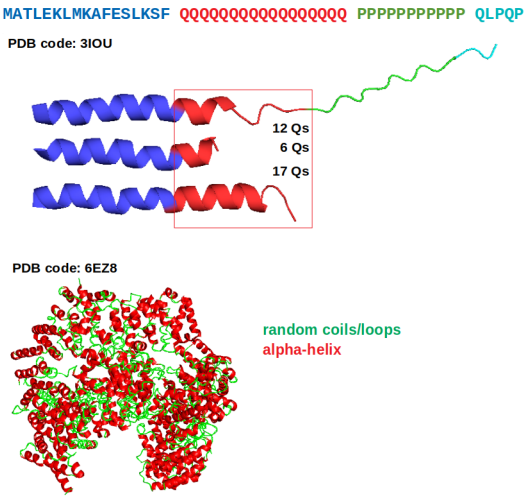

Figure 1. Secondary structure content for Ex.1-HTT (top) and 3138 sequence-length of HTT protein (bottom).

in computational studies are the structures encoded 3IO (3IOV, 3IOU, 3IOT, 3IOR, 3IO6, 3IO4),[22] and the 3138 sequence-length of HTT protein encoded 6EZ8.[47] Moreover, the N17 domain alone (having the sequence MATLEKLMKAFESLKSF) is also available under the PDB code 2LD0,[48] as is the crystal structure of N-terminal HTT with the insertion of three histidine residues (PDB codes 4FED, 4FEC, 4FE8).[46]

3.1.1. Wild-type and Mutant polyQ Structures. The concept that lies behind the severity of HD is based on the polyQ length, and it is considered to determine the "disease threshold". The presence of polyQ tracts longer than 36−40 glutamines (Qs) is associated with structural transitions from random coils to β-sheets.[25,27,37,49] In other words, it is considered that when there are higher numbers of Qs within the Ex1.-HTT, the protein elasticity also increases.[45,50,51] However, this hypothesis was not always supported. It was also shown that polyQ fragments shorter than the threshold tend to have the same behavior and to adopt similar structure after aggregation[52] as the ones with higher number of Q-residues. Additionally, the dimension of the polyQ tract seems to be more related to the mechanism of aggregate formation and not necessarily to their stability. On the other hand, it has been also shown that the kinetics of the linear addition of polyQ chains is not related to the dimension of polyQ stretch.[23,53,58]

There are several theoretical models of these aggregates that have been proposed that are highly consistent with the experimental data. Perutz et al. suggested that the Q side chains can establish H-bond interaction networks with the main chain atoms, because they are considered to be similar to the backbone units.[10,54,55] These interactions have the main role of stabilizing the polyQ aggregates.[10,11] The stabilization process was described by Esposito et al. assuming that the resulting β-sheets are antiparallel oriented so that the amine-group from one side chain can bind the carbonyl-group from the side chain associated with the subsequent turn.[56]

In terms of structural properties, most of the studies concluded that after aggregation polyQ sequences most likely follow the β-sheet structure.[10,24,57−61] On the other hand, another structural approach that has been consistent with X-ray diffraction data is the β-helix model. For soluble monomeric states of polyQ stretches with different lengths, the conformational changes vary among random coils,[23,25,26,49]

DOI: 10.1021/acschemneuro.9b00561
ACS Chem. Neurosci. 2020, 11, 105−120

α-helices (hairpin conformations belonging to HEAT repeats),[27,37] β-sheets,[27] and other extended types of helices.[62] All these conformational states were investigated using computational methods,[22,63−67] which provided a clear understanding of their stability,[65,68−71] the circular β-helix being the model that suggested a relationship between the increased number of Qs and the conformation in which the β-helices are kept stable (above approximately 30 Qs).[70] An additional proposed model is the Atkins's model where the H-bonds of the side chains inside the Qs explain their high-density packing.[72]

The conformational starting point of the Ex.1-HTT is an important issue that has to be taken into account prior each simulation. An extensively discussed hypothesis is that the shapes of polyQ structures are linearly correlated to the "disease threshold" effect. Contrarily, the polyQ's structural stability must be considered from multiple points of view: the shape of the initial structure, the number of Qs in the monomer, and the number of monomers.[71] In order to prove this, classical MD simulations[10,59,72−75] were performed with the main interest in mutant stability.[56,64,68−72,76−80] Although these models have been proposed to explain when and how exactly the polyQ aggregation takes place, because of the large variety of possible explanations and the plausible contradictions between the studies, this subject still remains unclear and consequently, widely discussed.

3.1.2. Structural Behavior Outside the PolyQ Tract. As previously mentioned, the first approach for polyQ aggregation was proposed to be only through the accumulation of the polyQ stretches.[81−84] In contrast, other results suggested that the external regions of the glutamine tract are able to interact with each other, promoting and regulating the aggregation process.[85,86]

Previous studies[65,70] have demonstrated that the N-terminal domain (N17) is also responsible for protein fibrillation due to several interactions with different cellular partners and changes in nucleation of aggregation. Although N17 is considered to exist in solution in equilibrium, the secondary and tertiary structures of different conformers are still not well-defined. The formation of fibrils was described by the proposed model of N17 adopting a helical fold upon its interaction with other cellular and subcellular partners.[87]

Other studies proposed the aggregation pathway as being dependent principally on N17 and involving different intermediates.[30,88] This kinetic mechanism involves the formation of certain oligomers consisting of N17 domains into their core, while the polyQ stretches are defined on the surface. With the increased number of Qs, the entire structure decompacts leading to a rearrangement of the oligomers into amyloid-like fibrils. These amyloid-like structures are able to spread through monomer addition.[30,88] Furthermore, upon increase of the polyQ length, the N17 tract is likely to form β-sheet arrangement. The side-by-side constructed regions are believed to be related not only to the polyQ sequences and N17 terminals but also to the polyP domains.[87]

Truant et al. and Atwal et al. have demonstrated that a single mutation in the N17 region (at the serine residue[85] and at the eighth huntingtin residue represented by methionine, which was mutated to proline, M8P mutation[89]) was able to break the formation of the helical structure with a complete disappearance of the visible polyQ aggregates.[85,89] The deletion of N17 residues reduces the polyQ tract aggregation because the clustering process seems to be accelerated by α-helical structure and hydrophobicity of the N17.[30]

The attention on the polyP region was clearly directed by the hypothesis that it may protect the polyQ conformation.[90] This protective behavior goes against the conformational collapse of the polyQs by keeping the structures soluble.[37,91] The influence of the polyP tract is also related to the disease's toxicity through the C-terminal region.[37,22] Over the years, the role of the flanking regions was associated mostly with the toxicity modulation of the m-HTT. On the other hand, it was also suggested that the m-HTT's toxicity may be related to the biochemical nature of the polyQ tracts, which are genetically toxic sequences, while their destructive effect increases with the number of CAG repeats.[92]

A recent article[45] emphasized that the polyQ predisposition to adopt β-sheet conformation increases as the numbers of Qs increases. According to the study, the β-sheet conformation was not stable in models represented with fewer polyQs. Also, the flanking regions appeared to alter the polyQ's aggregation. An antagonistic effect on the process was described upon N17's removal, which decreases the aggregation development, while the polyP region prevented it completely. The main conclusion of the study was that the critical length needed for Ex.1-HTT aggregation would be ≥40 Q residues for disease onset. MD simulations of eight different models of Ex.1-HTT were carried out in this study for 500 ns. The Q lengths of the models varied between 27 and 50. For Q27 and Q50, additional sequence of P11 was added.[45]

The residue fluctuations in the study of Priya et al. were assessed through RMSF graphs from which it was concluded that for most of the residues the values were larger than 0.5 nm, consequently belonging to flexible regions. The polyQ tracts with 50 Q residues presented a value of 1.27 nm, while the structures with Q34−36 and Q40 showed also high fluctuations up to 1.14 nm. RMSF values for the flanking sequences were not greater than 0.9 nm, although the value remains high. The N-terminal domain and the polyP region from the Q50P11 model presented larger variations than the ones from Q27P11 model, especially at the level of the proline residues, inducing less conformational stability.[45] Thus, as was expected, an increase in the number of the glutamine residues inside the HTT protein also triggers an increase in the protein's flexibility.[45,50,51]

The polyP region is considered to be an important asset in the conformational maintenance of the polyQ structures. It is considered that the inhibitory effect of the polyP residues depends on its length; therefore, it has been demonstrated that at least five proline molecules are required in order to have a decrease in the aggregation process.[88]

On the other hand, the spot of interaction is also a matter of importance. For example, the addition of a polyP tract to the N-terminal domain of the polyQ was not seen to have any impact on the aggregation,[37] but its presence in C-terminal domain inhibits the formation of the β-like conformations, while its absence induces β-sheet formation.[45,87] Another study has proposed the hypothesis that the polyP tracts actually protect cells against toxicity by preventing or inhibiting aggregation.[93] An additional assumption that might be helpful for studying the protein−protein interactions is that the polyP regions act as active binding sites for other HTT interacting proteins.[50]

3.2. Conformational Dynamics. Valuable understanding of the structural and dynamical properties of the polyQ tracts

DOI: 10.1021/acschemneuro.9b00561
ACS Chem. Neurosci. 2020, 11, 105−120

with different number of Qs in different oligomeric states can be achieved by using different computational approaches,[94,95] the most common being classical MD simulations.[95−98] However, as it was mentioned before, the complexity of the large intrinsically disordered proteins and also the limited computational resources have provided mixed results in terms of structural conformations of the mutant, even if different simulation techniques such as discrete MD engines, implicit solvents, and coarse-grained (CG) models were used. The main contradiction found in the literature is related to the secondary structure. Some articles suggested that the monomeric state of Ex.1-HTT is dominated by α-helical profiles,[40,52,99,100] while other studies reported that β-sheet formation rate in monomers increases with the increased number of Qs.[40,87]

The structural stability of monomers and oligomers implicated in polyQ structures was investigated through atomistic MD simulations on different models presenting polyQ length lower and higher than the disease threshold.[71] From classical MD studies,[77−79,101] it was shown that β-helices having three turns tend to be unstable in circular geometries but stable in triangular β-helix shape. Also, at the time of dimerization two-coiled triangular β-helices become stable, whereas individually they were considered to be unstable. These findings lead to the conclusion that for the initial aggregation point of HTT, 36 Qs are required, at least,[68] and that the complex stability increases with an increased number of rungs but still remains insensitive to the actual number of Q residues taking part in polyQ fragments.[102]

The contradictions at this level have offered a large variety of features to the huntingtin protein and encouraged researchers to focus on HD from its overall biological aspects[3,42,44,103] to polyQ tracts and the flanking region's involvement in the aggregation process.[53,104]

3.2.1. Structural Stability and Toxicity Development. A systematic all-atom MD study was performed on the full Ex1.-HTT by Kang et al., focused on different polyQ lengths, emphasizing the elongation effect of the polyglutamine tract and the connection between the CAG repeats and the disease pathology.[40] As previously discussed, an increase in the Q length leads to β-sheet conformation in Ex.1, with the ultimate effect of reducing contact between N-terminal and C-terminal fragments. This structural behavior leads to an enhanced compactness of the polyQ region, which is considered to be one of the two main reasons (the other reason is considered to be the aggregation alone) for the induced toxicity. The condensed conformational effects may be attributed to the changes in the interactions between HTT itself and other HTT proteins, as well as with their different binding partners.[40]

In partial agreement with other studies, the molecular dynamics simulations were conducted on the FASTA sequence: MATLEKLMKAFESLKFS**Q(*n*)**P(11)QLPQP(3)-QAQPLLPQPQP(10), where the *n* values of the polyQ tract constituted different types of models. Kang et al. used temperature replica exchange molecular dynamics (T-REMD)[105,106] in order to enhance the conformational free energy surfaces.[40] After 1 ns of equilibration, they carried out 500 ns per replica simulations increasing the temperature from 298 to 600 K. All their simulations were performed using GROMACS 5.0.5[107] and OPLS-AA/L force field.[108]

The radius of gyration (R_g) scaling exponent for polyQ domains in Ex.1-HTT was around 0.22 according to Kang et al., in contrast to typical globular proteins with an R_g of 0.33. This consistent decrease in R_g value implies a loss of structure flexibility. Hence, the proteolysis processes of m-HTTs become altered; consequently the degradation mechanisms are restrained, followed by mutant accumulation in brain cells.[40,109]

Another study mentioned in the previous sections is the one conducted by Rossetti et al., in which GROMACS software was also used for the 20 ns simulations. In comparison to the study of Kang et al., in this study the temperature was kept around 300 K and the GROMOS96 force field was selected because of its explicit representation of acidic hydrogen atoms.[71] Similarly to other studies, the systems were solvated with the simple point-charge (SPC) water model in a periodic box (rectangular in this case; cubic in other studies).[110] The long-range electrostatic interactions were usually treated with particle mesh Ewald (PME) method with the real part of calculations set at 0.9 nm. The cutoff radius for the Lennard-Jones (LJ) interactions was also set to 0.9 nm.[40]

The "structural stability" concept was driven over the years by different physical foundations, like the overall number of hydrogen bonds,[70] the β-strandlike shapes, and the obtained values of backbone dihedral angles[65,68] and, the most deliberated criteria, the conservation of a specific conformation.[68]

In 2008, Rossetti et al. followed a different point of view regarding the "disease threshold" and the importance of a stable structural conformation. The shape has not always had an impact on the content. To be more specific, they have concluded that the structural stability and oligomeric states are not affected by their shape. Moreover, the secondary structure does not depend on the number of Qs present in monomers.[71] Another theoretical study[70] stated on the other hand, that "the stability of an aggregate should be regulated by the structural stability of its component monomers". This statement was established after 1 ns of MD simulations using AMBER force field.[111] The experiment time-scale appeared not to be sufficient for a valid conclusion.[70]

For longer time-scale simulations, the secondary structure of oligomers with 4 monomers of 40 Qs and the ones with 8 monomers of 25 Qs were almost the same.[71] This result was highly consistent with another study that revealed no structural differences between the long polyQ aggregates and the short ones.[92] The structural stability has no direct effect on the structural threshold hypothesis, because the conformations of the polyQ tracts are not always specific when they achieve pathological length. Hence, the overall stability is being controlled just by the number of the additional monomers (because of the H-bond network formed between the backbone atoms). At this point, the only equitable connection between the polyQ length and the toxicity itself, may be described by the fact that for longer polyQ tracts, the aggregation process might be faster,[71] therefore inducing a considerable risk for toxicity.

Another computational study focused on different polyQ length (from Q16 to Q80) is that reported by Gomez-Sicilia et al., whose main purpose was to determine "the structural and mechanical properties of the polyQ structures" and to describe, with further clarification, the conformational polymorphism.[112] Bias exchange molecular dynamics (BEMD) was used to generate polyQ structures and to characterize their conformations, a technique that was used in other studies as well.[113] GROMACS software package and AMBER99SB force field were used. The authors' conclusion was that the

DOI: 10.1021/acschemneuro.9b00561
ACS Chem. Neurosci. 2020, 11, 105−120

mechanical stability is unrelated to the structure's conformation. Large mechanical stability was seen for structures with large secondary structure content but also for structures with secondary structure of 30% (percentage of residues correlated with helices, strands, and H-bond turns). "Knotted structures" (clustered spots) were observed for n = 60 (Q number), and the clustered structures were about 36 Qs in size, the last number being considered the disease threshold.[112]

The structural stability and the aggregation properties were extensively discussed in the literature.[65,114,115] The conformational landscape presented in the three studies, structures turning into steric zippers and β-helix, was not in agreement with the conformational states found by Gomez-Sicilia et al.,[112] because they considered monomers and not dimers.

3.2.2. The Polymerization Kinetics. Although polyQ tracts are considered to change their behavior with the addition of glutamine residues and to aggregate in an abnormal manner, the polyQ length is now considered to affect the nucleation−growth polymerization kinetics of those aggregates and not necessarily their stability.[71,92] The kinetics involve first a transition from random coil to β-sheet conformation on an individual monomer, at this point forming the actual aggregation seed, which is subsequently multiplied until it reaches the toxicity threshold.[23,58,106] According to this hypothesis, Rossetti et al. have speculated that the aggregation process indeed increases upon increasing the number of Q residues. Although the simulation results are in high agreement with this assumption, further investigations are necessary[71] especially because, in contrast, it has been shown that once the aggregation seed is formed, the number of glutamines have no impact on the elongation process.[58] This ultimate contradiction might be due to the limited time of the simulation (20 ns); although longer than the one reported in previous articles,[70] it is still too short for an accurate time-dependent progression of the process.[71]

3.2.3. The Compact Model and Cerebral Inclusion Formation. An outstanding question that might help to describe the disease's phenotype would be are those cerebral inclusions an actual proof of toxicity as an ultimate effect of the mutation or is their formation just a defensive mechanism?

In the study of Zhang et al. the stability of certain compact polyQ structures was established throughout 10 ns MD simulations.[117] The role of the H-bonding network in stabilization of the compact β-structure was assessed, as well. The study was based on the hypothesis already mentioned before, that the formation of highly compact β conformation[82,83] represents a prerequisite for the toxicity induction.[117] Consecutive β-strands of the same peptide (PGQ6 and PGQ12) were modeled, solvated, equilibrated, and simulated over a 20 ns simulation period. As in any other theoretical study, before the MD runs, the input models were subjected to energy minimization (in 5000 steps) with the conjugate gradient algorithm incorporated in the program. Afterward, the models were solvated into a rectangular box with TIP3 water molecules. After the solvation, another minimization step was applied to the entire system. The temperature of the system was 300 K acquired in 10 000 steps. All-atom MD simulations were performed in the study[117] with CHARMM 22/27 force field and the NAMD simulation program.[116]

The results suggested a loss in the extended β-sheet conformation, an interesting result if we consider the other studies in which this type of conformation is highly preserved at the level of the polyQ tracts. According to experimental data, it seems that upon altering the polyQ length inside the β-strands of the same mutant Ex.1-HTT, the formation of the aggregates in brain cells decreases but the structures remain toxic even if they are still soluble.[117]

3.3. Interatomic Interactions. In classical MD method, the atoms move according to the Newton's law and on a predefined potential energy surface, the interatomic interactions being characterized by empirical force fields. Nonetheless, this theoretical technique implies a huge disadvantage in terms of simulation time scale. In explicit water, MD simulations are limited to hundreds of nanoseconds. In contrast, the biological concepts are developed on larger time scales; thus the most relevant results may be achieved by combining the MD simulations with enhanced computational techniques.[110,118] In addition, the use of simplified interaction potentials might be required.[95,97,119]

Certainly, the electronic structure techniques are much more computationally demanding than the classical MD simulations. This limitation comes with the system's size restriction to hundreds of atoms and also the time scale of *ab initio* MD being limited to tens of picoseconds.[110,119,120] A solution to this drawback would be to treat the systems by using hybrid techniques such as quantum-classical (QM/MM) MD simulations (classical and *ab initio* MD). Several computational studies[105,121−124] have used the QM/MM method to understand the electronic factors that contribute to the β-sheet conformational stability, an issue that has become of a fundamental interest in the research field of neurodegeneration diseases.[119] In addtion, long-range interactions were demonstrated to have a greater impact on β-sheet stability, the H-bond lengths being very sensitive to these interactions and following valuable changes into the molecular geometry.[119,125,126]

The aggregation properties of the polyQ chains were studied in correlation with the initial aggregation seed formation,[88] together with the implication of the flanking regions at the level of the first exon of m-HTT protein. In the study conducted by Wetzel et al., the nucleated growth polymerization model was initially based only on the connection between the disordered polyQs, leading to highly ordered β-sheet structures that were clearly seen in the experimental data as β-like fibrils.[28,101,119]

Another common approach used to describe the mutation's initiation at the atomic level is based on the so-called coarse grain (CG) models, where groups of atoms are described as a single bead.[118] A coarse-grained system makes reference to a simplified system in which the individual atoms are represented by "pseudo-atoms" containing groups of "real atoms", for example, an entire amino-acid residue. The simplest CG model includes three types of beads: hydrophilic, hydrophobic, and neutral. However, in order to characterize the aggregation process in which the cooperativity effects are crucial, CG models must have "special beads" that can account for H-bond evolution.[97] As it was expected, the CG method allows enlarging the simulation time-scale, but it might lose, at the same time, the correctness of the atomistic description.[110] Among the theoretical methods used in the studies on neurodegenerative diseases, discrete molecular dynamics (DMD) represents another efficient MD technique based on simplified interparticle potentials.[95,110] DMD was selected for use to emphasize the importance of the folding behavior of a chimeric monomer containing polyQ repeats. The coopera-

DOI: 10.1021/acschemneuro.9b00561
ACS Chem. Neurosci. 2020, 11, 105−120

tivity appeared to decrease for polyQ structures with Q tracts above the pathogenic threshold.[110]

Barton et al. have demonstrated that the dimer formation is based on the interglutamine H-bonding interaction.[127] The H-bond and hydrophobic interactions are the most important issues that must be considered for an accurate description of the polyQ aggregation process and its progression into a folded conformation.[77−79]

The aggregation of different polyQ structures of different lengths was also investigated via replica exchange (RE) MD using a simplified force field and a higher temperature range between 241 and 800 K.[105,114] In this article, the aggregation kinetics of several polyQ monomers and dimers with lengths between 30 and 50 residues were studied, and it was concluded that in case of monomers, the structure varied from α-helices to random coils without the formation of β-strands. On the other hand, for dimers, antiparallel β-sheets and circular and triangular β-helices appeared after the initial random coil formation. These drastic structural changes may lead to toxic oligomer initiation.[110,114]

Kelley et al.[99] have proposed two possible nucleation mechanisms. The first is based on the changeover between the two-helix and single-helix shape of the N17 and the second one is based on the direct interaction between the N17 and the polyQ chains.[104,110,128] With respect to the first mechanism, the most populated stable state of N17 was found, via MD simulations, to be particularly a two-helix bundle, even though other structural configurations still adopt the single-helix pattern.[99]

3.3.1. Polyglutamine Expansion, the Role of Flanking Regions, and Amyloid-Like Structures. A common ground for Alzheimer's, Parkinson's, and Huntington's diseases is the (structural) formation of amyloid-like fibrils.[53,129,130] It has been demonstrated that even the WT structures tend to form fibrils. The aggregation process seems to take place, under specific conditions, for pathogenic but also for nonpathogenic polyQ tracts.[58,131,132] As was mentioned in the previous sections, the most widely discussed hypothesis is that fibrils are being formed because of their linear correlation to the polyQ length. Also, a longer glutamine-repeat tract accelerates the aggregation process.[23,37,58,106,133−135] But from a morphological point of view, experimental studies demonstrated that fibrillar structures, including the amyloid formation stages for m-HTT, present distinctive aggregation conditions and, consequently, different aggregation behaviors.[30,40,135−143]

The polyglutamine's direct implication in fibril formation has been questioned over recent years, while the flanking sequences are now believed to play a crucial role in the aggregation mechanism.[30,32,33,49,87,104,142,144−149] The aggregation rates were observed to decrease when polyP residues were added to the C-terminal domain,[32,37,150] these results being associated with great impact on the toxicity level. In contrast, the addition of polyP segments to the N-terminal domain does not affect the aggregation process.[37,53]

The intermolecular interactions between N17 and polyQ tracts and intramolecular interactions (N17−N17) were investigated with the use of computational methods.[151] Those 17 amino acids from the N-terminal domain are considered to encourage the interaction between m-HTT monomers through a self-association process; therefore the oligomeric states facilitate fibril formation[29,30,33,142,152,153] and, of course, increase the aggregation rate.[30,35,89,93,139,142,148] Another essential role of the N-terminal domain is that it functions as "a lipid binding domain"[48,148,154,155] presenting high binding affinity for curved membranes.[156−158]

The proposed idea that the monomeric states can bind predefined fibrils was characterized through atomistic calculations in 2011 by Straub and Thirumalai. Their modeled system consisted of interactions between amyloid β peptide and fibrils, and they concluded that the nonstructured monomers suffer structural transitions in order to fit the oligomer's conformation, therefore presenting an elongation of the oligomers.[159] In the same year, another study[160] stated that these conformational fittings also occur when monomers interact with dimers.[160,161]

Binding partners might be involved in the generation of a large variety of helical structures, but also other post-translational modifications (phosphorylation and acetylation) may exert great influence on HTT/m-HTT aggregation.[53,161−163] For example, phosphorylation of the N-terminal domain, at T3, S13, or S16, was associated with a reduced toxicity level.[164−170] Likewise, the acetylation of N17 was found to reduce the aggregation states and also to decrease the protein's binding affinity to lipid membranes.[171] Granting all this, there are certain physicochemical properties that must be considered, in terms of curvature, elasticity, fluidity, and surface charges, when HTT/m-HTT interacts with lipid membranes.[172−175]

3.4. Protein−Protein Interaction. The experimental results emphasized the role of the wild-type HTT protein to protect neuronal cells against apoptotic stress.[176] Changes in this antiapoptotic role is considered to alter the proper communication between neurons, and as a consequence, a further alteration between HTT and other binding partners might be involved.[177−179] The increased number of polyQ tracts promotes mass accumulation incorporating the polyQ fibrils.[141] When the m-HTT interacts with other proteins, a colocalization of the structures takes place usually because of the mutated sections, leading to an abnormal distribution of the connected complexes.[180]

The research report of Gopalakrishnan et al. characterized crucial aspects of the dynamic behavior of HTT protein using molecular docking and MD simulations and provided valuable insights into the structural changes involved in HD.[179] They have docked the SH3 domain of SH3GL3 protein with three different models of HTT protein: HTT with 0Q, which was the control model of the experiment, HTT with 17Qs (wt-HTT), and HTT with 36Qs (m-HTT). The SH3 domain of SH3GL3 was chosen because it is considered to interact with the HTT protein.[179]

The simulation methodology was almost the same as in the previous MD studies focused on HD. The GROMACS 4.0.5 software was used to perform the MD simulations. Prior to the 10 ns of *mdrun*, the polyQ proteins alone and the docked complexes were solvated with SPC water model in a cubic box. The system was electrically neutral after the addition of the chloride ions. The equilibration steps were made for 500 ps (NVT) and 1000 ps (NPT) at 300 K. The equilibrated systems were then subjected to MD simulation (for 10 ns) at 300 K, without any constraint.[179]

As mentioned before, interactions between HTT and SH3GL3 lead to colocalization of the HTT−SH3GL3 complex in the neuronal cytoplasm, which implies a deficit of the docked complex at the level of the presynaptic regions[181] and a high potential for disease onset. The results of this study showed the least interaction, as it was expected, between the

DOI: 10.1021/acschemneuro.9b00561
ACS Chem. Neurosci. 2020, 11, 105−120

control (0Q) and the SH3GL3, compared to the interaction with 17Q and 36Q models. But the complex with 36Qs (36Q−SCH3GL3) presented the highest interaction fluctuations among the models, and in agreement with the study of Kim et al., the mutant−SH3 complex showed the highest flexibility due to the polyQ tract length and the presence of polyP rich domains.[22,179]

Structural rearrangements were also seen to be induced when HTT monomers interact with the molecular tweezer CLR01,[182] which is known to inhibit the accumulation of several amyloid-like proteins and shows a high affinity for lysine residues binding that part of the N17 domain involved in m-HTT polymerization.[104,183,184] In order to examine the molecular effects of this interaction, classical MD and REMD, as well as QM/MM calculations, were performed. The input structure consisted of 55 Qs,[182] and the results were divided into individual parts of the mHTT-Ex.1. N17 domain can bind simultaneously three CLR01 molecules. At the mutation level (in the presence of CLR01), MD trajectories at 300 K did not show changes in the secondary structure of the polyQ55 tract. However, without CLR01, N17 showed 81% α-helical conformation, while bound to CLR01 it presented 71% helical secondary structure conformation, this preferential arrangement being in high agreement with other studies.[52,99] This contradictory behavior between N17 and polyQ tract might suggest that CLR01 has no direct impact on inclusion formation in the body but can be considered as a good strategy for slowing down the aggregation kinetics (at the level of N17 domain) and therefore inhibiting the fibrillar structure's evolution.[182]

As a general conclusion to the polyQ interaction kinetics, the previously discussed hypothesis that the binding of HTT protein to its partners is mostly related to the polyQ chain length may be a key factor in resolving the structural and functional questions, not only related to other binding structures but also to the binding between the mutants themselves. On the other hand, the key factor for decreasing the aggregation processes is not necessarily related to the polyQ itself but to the N17 terminal domain considered essential for HTT-interacting complexes.

3.5. Novel Approach for HD Treatment. In 2018, Caterino et al. summarized the experimental results focused on "the multiple facets of the HTT protein", together with the impact on post-translational modifications of the m-HTT.[185] A valuable experimental finding that can be explored with the use of MD techniques is the one regarding aptamer-binding HTT gene. It is considered that oligonucleotides are able to inhibit pathological pathways of HD.[186−189] DNA aptamers possess an essential folding behavior required for molecular recognition. This leads to their ability to bind a wide range of proteins, ions, viruses, and even cellular compartments.[185,190−192] Nonetheless, even though aptamer-binding complexes might present an excellent strategy for HD treatment, this research topic is still at its early stage of development and consequently, being treated just as preliminary data.[185]

4. CONCLUSIONS

Despite the relevant computational findings, HTT's function and the polymerization process that describes how the mutation is formed still remains unknown. In general, it is strongly believed that as the Q-length increases the polyQ structures tend to adopt more β-sheet conformation. The polyglutamine tracts are not the only ones related to this type of conformation. The N17 domains can also form more β-like structures as the Q-length increases.

Another structural behavior that must be taken into account is that the increased number of Q residues in the polyQ tracts leads to condensed structures with highly compact distributed residues in the polyQ regions. The shape of the m-HTT becomes more spherical as the number of the Q residues increases.

Although several theoretical studies proved the existence of different aggregation pathways, the detailed mechanism regarding the polyQ monomer's assembly remains elusive. The thermodynamic stability of the m-HTT may not be related to the aggregation itself. The most debated assumption would be that the aggregate stability has actually nothing to do with the number of Qs in the m-HTT but with the initial stage of the seed nucleation. Moreover, the length-dependent toxicity threshold may be associated with the speed of the aggregation mechanism, which increases for longer polyQ tracts. However, these findings contradict the initial hypothesis that the aggregation speed is dependent on the 36Qs threshold.

With respect to the theoretical approaches, there are still several limitations in obtaining detailed behavior of polyQ aggregation. The computational techniques mentioned in this review are very demanding in terms of accessible computational time for full atomistic simulations, and in some cases, because of the deficiencies in force field parametrization, simulating the aggregation of large biological structures at a relevant scale may be not possible. CG method is considered to be a suitable tactic for large system simulations at longer time scale, but in this case, the atomistic description might be compromised.

Ultimately, several of the presented studies have decided in this aspect that the development of an appropriate multiscale computational method based on a hybrid methodology (CG and force field based MD) may be really useful for a proper biochemical characterization of the inclusion formation in brain cells.

AUTHOR INFORMATION

ORCID

Vasile Chiş: 0000-0002-0935-4134

Author Contributions

S.N.M. designed the analysis, collected the data, analyzed data, and wrote the original draft. V.C. conceived and designed the analysis, analyzed data, and revised the manuscript.

Funding

S.N.M. acknowledges the support of the CNCS-UEFISCDI Romania, grant PN-III-P1-1.1-TE-2016-0628. V. Chiş acknowledges the support of the CNCS-UEFISCDI Romania, grant PN-III-P4-ID-PCCF-2016-0112.

Notes

The authors declare no competing financial interest.

REFERENCES

(1) Ross, C. A., and Tabrizi, S. J. (2011) Huntington's disease: from molecular pathogenesis to clinical treatment. *Lancet Neurol. 10* (1), 83−98.

(2) Frank, S. (2014) Treatment of Huntington's disease. *Neurotherapeutics 11* (1), 153−60.

(3) Saudou, F., and Humbert, S. (2016) The biology of huntingtin. *Neuron 89* (5), 910−926.

DOI: 10.1021/acschemneuro.9b00561
ACS Chem. Neurosci. 2020, 11, 105−120

(4) Veldman, M. B., and Yang, X. W. (2018) Molecular Insights into Cortico-striatal Miscommunications in Huntington's Disease. *Curr. Opin. Neurobiol. 48*, 79−89.
(5) Sharp, A. H., Loev, S. J., Schilling, G., Li, S. H., Li, X. J., Bao, J., Wagster, M. V., Kotzuk, J. A., Steiner, J. P., Lo, A., Hedreen, J. C., Sisodia, S. S., Snyder, S. H., Dawson, T. M., Ryugo, D. K., and Ross, C. A. (1995) Widespread expression of Huntington's disease gene (IT15) protein product. *Neuron 14*, 1065−1074.
(6) Gutekunst, C. A., Levey, A. I., Heilman, C. J., Whaley, W. L., Yi, H., Nash, N. R., Rees, H. D., Madden, J. J., and Hersch, S. M. (1995) Identification and localization of huntingtin in brain and human lymphoblastoid cell lines with anti-fusion protein antibodies. *Proc. Natl. Acad. Sci. U. S. A. 92*, 8710−8714.
(7) Ellisdon, A. M., Thomas, B., and Bottomley, S. P. (2006) The two-stage pathway of ataxin-3 fibrillogenesis involves a polyglutamine-independent step. *J. Biol. Chem. 281*, 16888−16896.
(8) Gray, M., Shirasaki, D. I., Cepeda, C., Andre, V. M., Wilburn, B., Lu, X. H., Tao, J., Yamazaki, I., Li, S. H., Sun, Y. E., Li, X. J., Levine, M. S., and Yang, X. W. (2008) *J. Neurosci. 28*, 6182.
(9) Bates, G. P. (2005) History of genetic disease: the molecular genetics of Huntington disease - a history. *Nat. Rev. Genet. 6* (10), 766−73.
(10) Perutz, M. F. (1994) Polar Zippers - Their Role in Human-Disease. *Protein Sci. 3* (10), 1629−1637.
(11) Perutz, M. F., Johnson, T., Suzuki, M., and Finch, J. T. (1994) *Proc. Natl. Acad. Sci. U. S. A. 91*, 5355.
(12) Imarisio, S., Carmichael, J., Korolchuk, V., Chen, C. W., Saiki, S., Rose, C., Krishna, G., Davies, J. E., Ttofi, E., Underwood, B. R., and Rubinsztein, D. C. (2008) Huntington's disease: from pathology and genetics to potential therapies. *Biochem. J. 412* (2), 191−209.
(13) Miller, J., Arrasate, M., Brooks, E., Libeu, C. P., Legleiter, J., Hatters, D., Curtis, J., Cheung, K., Krishnan, P., Mitra, S., Widjaja, K., Shaby, B. A., Lotz, G. P., Newhouse, Y., Mitchell, E. J., Osmand, A., Gray, M., Thulasiramin, V., Segal, M., Yang, X. W., Masliah, E., Thompson, L. M., Muchowski, P. J., Weisgraber, K. H., Finkbeiner, S., and Saudou, F. (2011) *Nat. Chem. Biol. 7*, 925.
(14) Binette, V., Cote, S., and Mousseau, N. (2016) Free-Energy Landscape of the Amino-Terminal Fragment of Huntingtin in Aqueous Solution. *Biophys. J. 110* (5), 1075−1088.
(15) Tobin, A. J., and Signer, E. R. (2000) Huntington's disease: the challenge for cell biologists. *Trends Cell Biol. 10*, 531−6.
(16) Ross, C. A. (2002) Polyglutamine pathogenesis: emergence of unifying mechanisms for Huntington's disease and related disorders. *Neuron 35*, 819−22.
(17) Rubinsztein, D. C. (2002) Lessons from animal models of Huntington's disease. *Trends Genet. 18*, 202−9.
(18) Cha, J. H. (2007) Transcriptional signatures in Huntington's disease. *Prog. Neurobiol. 83*, 228−48.
(19) Takahashi, T., Katada, S., and Onodera, O. (2010) Polyglutamine diseases: where does toxicity come from? what is toxicity? where are we going? *J. Mol. Cell Biol. 2*, 180−91.
(20) Kim, M. (2013) Beta conformation of polyglutamine track revealed by a crystal structure of Huntingtin N-terminal region with insertion of three histidine residues. *Prion 7* (3), 221−228.
(21) Temussi, P. A., Masino, L., and Pastore, A. (2003) From Alzheimer to Huntington: why is a structural understanding so difficult? *EMBO J. 22*, 355−61.
(22) Kim, M. W., Chelliah, Y., Kim, S. W., Otwinowski, Z., and Bezprozvanny, I. (2009) Secondary structure of Huntingtin amino-terminal region. *Structure 17*, 1205−12.
(23) Chen, S., Berthelier, V., Yang, W., and Wetzel, R. (2001) Polyglutamine aggregation behavior in vitro supports a recruitment mechanism of cytotoxicity. *J. Mol. Biol. 311*, 173−82.
(24) Tanaka, M., Morishima, I., Akagi, T., Hashikawa, T., and Nukina, N. (2001) Intra- and intermolecular beta-pleated sheet formation in glutamine-repeat inserted myoglobin as a model for polyglutamine diseases. *J. Biol. Chem. 276*, 45470−45475.
(25) Masino, L., Kelly, G., Leonard, K., Trottier, Y., and Pastore, A. (2002) Solution structure of polyglutamine tracts in GST-polyglutamine fusion proteins. *FEBS Lett. 513*, 267−72.
(26) Bennett, M. J., Huey-Tubman, K. E., Herr, A. B., West, A. P., Jr., Ross, S. A., and Bjorkman, P. J. (2002) A linear lattice model for polyglutamine in CAG-expansion diseases. *Proc. Natl. Acad. Sci. U. S. A. 99*, 11634−11639.
(27) Nagai, Y., Inui, T., Popiel, H. A., et al. (2007) A toxic monomeric conformer of the polyglutamine protein. *Nat. Struct. Mol. Biol. 14* (4), 332−340.
(28) Wetzel, R. (2012) Physical chemistry of polyglutamine: intriguing tales of a monotonous sequence. *J. Mol. Biol. 421*, 466−490.
(29) Sahoo, B., Singer, D., Wetzel, R., et al. (2014) Aggregation behavior of chemically synthesized, full-length huntingtin exon1. *Biochemistry 53*, 3897−3907.
(30) Thakur, A. K., Jayaraman, M., Mishra, R., Thakur, M., Chellgren, V. M., Byeon, I. J. L., Anjum, D. H., Kodali, R., Creamer, T. P., Conway, J. F., Gronenborn, A. M., and Wetzel, R. (2009) Polyglutamine disruption of the huntingtin exon 1 N terminus triggers a complex aggregation mechanism. *Nat. Struct. Mol. Biol. 16* (4), 380−389.
(31) Liebman, S. W., and Meredith, S. C. (2010) Protein folding: sticky N17 speeds huntingtin pile-up. *Nat. Chem. Biol. 6*, 7−8.
(32) Darnell, G., Orgel, J. P. R. O., Meredith, S. C., and Pahl, R. (2007) Flanking polyproline sequences inhibit β-sheet structure in polyglutamine segments by inducing PPII-like helix structure. *J. Mol. Biol. 374*, 688−704.
(33) Jayaraman, M., Kodali, R., Wetzel, R., et al. (2012) Slow amyloid nucleation via α-helix-rich oligomeric intermediates in short polyglutamine-containing huntingtin fragments. *J. Mol. Biol. 415*, 881−899.
(34) Jayaraman, M., Mishra, R., Wetzel, R., et al. (2012) Kinetically competing huntingtin aggregation pathways control amyloid polymorphism and properties. *Biochemistry 51*, 2706−2716.
(35) Crick, S. L., Ruff, K. M., Pappu, R. V., et al. (2013) Unmasking the roles of N- and C-terminal flanking sequences from exon 1 of huntingtin as modulators of polyglutamine aggregation. *Proc. Natl. Acad. Sci. U. S. A. 110*, 20075−20080.
(36) MacDonald, M. E., Ambrose, C. M., Duyao, M. P., Myers, R. H., Lin, C., Srinidhi, L., Barnes, G., Taylor, S. A., James, M., Groot, N., MacFarlane, H., Jenkins, B., Anderson, M. A., Wexler, N. S., Gusella, J. F., Bates, G. P., Baxendale, S., Hummerich, H., Kirby, S., North, M., Youngman, S., Mott, R., Zehetner, G., Sedlacek, Z., Poustka, A., Frischauf, A. M., Lehrach, H., Buckler, A. J., Church, D., Doucette-Stamm, L., O'Donovan, M. C., Riba- Ramirez, L., Shah, M., Stanton, V. P., Strobel, S. A., Draths, K. M., Wales, J. L., Dervan, P., Housman, D. E., Altherr, M., Shiang, R., Thompson, L., Fielder, T., Wasmuth, J. J., Tagle, D., Valdes, J., Elmer, L., Allard, M., Castilla, L., Swaroop, M., Blanchard, K., Collins, F. S., Snell, R., Holloway, T., Gillespie, K., Datson, N., Shaw, D., and Harper, P. S. (1993) A novel gene containing a trinucleotide repeat that is expanded and unstable on Huntington's disease chromosomes. *Cell 72* (6), 971−983.
(37) Bhattacharyya, A., Thakur, A. K., Wetzel, R., et al. (2006) Oligoproline effects on polyglutamine conformation and aggregation. *J. Mol. Biol. 355*, 524−535.
(38) Côté, S., Wei, G., and Mousseau, N. (2012) All-atom stability and oligomerization simulations of polyglutamine nanotubes with and without the 17-amino-acid N-terminal fragment of the Huntingtin protein. *J. Phys. Chem. B 116*, 12168−12179.
(39) Ruff, K. M., Khan, S. J., and Pappu, R. V. (2014) A coarse-grained model for polyglutamine aggregation modulated by amphipathic flanking sequences. *Biophys. J. 107*, 1226−1235.
(40) Kang, H., Vázquez, F. X., Zhang, L., Das, P., Toledo-Sherman, L., Luan, B., Levitt, M., and Zhou, R. (2017) Emerging β-sheet rich conformations in super-compact Huntingtin exon-1 mutant structures. *J. Am. Chem. Soc. 139* (26), 8820−8827.
(41) Hoop, C. L., Lin, H. K., Kar, K., Hou, Z., Poirier, M. A., Wetzel, R., and van der Wel, P. C. A. (2014) Polyglutamine Amyloid Core Boundaries and Flanking Domain Dynamics in Huntingtin Fragment

DOI: 10.1021/acschemneuro.9b00561
ACS Chem. Neurosci. 2020, 11, 105−120

Fibrils Determined by Solid-State Nuclear Magnetic Resonance. *Biochemistry 53*, 6653−6666.
(42) Marques Sousa, C., and Humbert, S. (2013) Huntingtin: here, there, every-where! *J. Huntington's Dis. 2*, 395−403.
(43) Saudou, F., Finkbeiner, S., Devys, D., and Greenberg, M. E. (1998) Huntingtin Acts in the Nucleus to Induce Apoptosis but Death Does Not Correlate with the Formation of Intranuclear Inclusions. *Cell 95* (1), 55−66.
(44) Jimenez-Sanchez, M., Licitra, F., Underwood, B. R., and Rubinsztein, D. C. (2017) Huntington's Disease: Mechanisms of Pathogenesis and Therapeutic Strategies. *Cold Spring Harbor Perspect. Med. 7*, No. a024240.
(45) Priya, B. S., and Gromiha, M. M. (2019) Structural insights into the aggregation mechanism of huntingtin exon 1 protein fragment with different polyQ lengths. *J. Cell. Biochem. 120*, 10519−10529.
(46) Kim, M. (2013) Beta conformation of polyglutamine track revealed by a crystal structure of Huntingtin N-terminal region with insertion of three histidine residues. *Prion 7* (3), 221−228.
(47) Guo, Q., Bin Huang, Cheng, J., Seefelder, M., Engler, T., Pfeifer, G., Oeckl, P., Otto, M., Moser, F., Maurer, M., Pautsch, A., Baumeister, W., Fernandez-Busnadiego, R., and Kochanek, S. (2018) The cryo-electron microscopy structure of huntingtin. *Nature 555* (7694), 117−120.
(48) Michalek, M., Salnikov, E. S., and Bechinger, B. (2013) b Structure and Topology of the Huntingtin 1−17 Membrane Anchor by a Combined Solution and Solid-State NMR Approach. *Biophys. J. 105*, 699−710.
(49) Altschuler, E. L., Hud, N. V., Mazrimas, J. A., and Rupp, B. (1997) Random coil conformation for extended polyglutamine stretches in aqueous soluble monomeric peptides. *J. Pept. Res. 50*, 73−75.
(50) Neveklovska, M., Clabough, E. B., Steffan, J. S., and Zeitlin, S. O. (2012) Deletion of the huntingtin proline-rich region does not significantly affect normal huntingtin function in mice. *J. Huntington's Dis. 1* (1), 71−87.
(51) Caron, N. S., Desmond, C. R., Xia, J., and Truant, R. (2013) Polyglutamine domain flexibility mediates the proximity between flanking sequences in huntingtin. *Proc. Natl. Acad. Sci. U. S. A. 110* (36), 14610−14615.
(52) Długosz, M., and Trylska, J. (2011) Secondary structures of native and pathogenic huntingtin N terminal fragments. *J. Phys. Chem. B 115* (40), 11597−11608.
(53) Adegbuyiro, A., Sedighi, F., Pilkington, A. W., IV, Groover, S., and Legleiter, J. (2017) Proteins containing expanded polyglutamine tracts and neurodegenerative disease. *Biochemistry 56* (9), 1199−1217.
(54) Perutz, M. F. (1999) Glutamine repeats and neurodegenerative diseases: molecular aspects. *Trends Biochem. Sci. 24* (2), 58−63.
(55) Perutz, M. F., and Windle, A. H. (2001) Cause of neural death in neurodegenerative diseases attributable to expansion of glutamine repeats. *Nature 412* (6843), 143−144.
(56) Esposito, L., Paladino, A., Pedone, C., and Vitagliano, L. (2008) Insights into structure, stability, and toxicity of monomeric and aggregated polyglutamine models from molecular dynamics simulations. *Biophys. J. 94* (10), 4031−4040.
(57) Bevivino, A. E., and Loll, P. J. (2001) An expanded glutamine repeat destabilizes native ataxin-3 structure and mediates formation of parallel b-fibrils. *Proc. Natl. Acad. Sci. U. S. A. 98* (21), 11955−11960.
(58) Chen, S. M., Berthelier, V., Hamilton, J. B., O'Nuallai, B., and Wetzel, R. (2002) a. Amyloid-like features of polyglutamine aggregates and their assembly kinetics. *Biochemistry 41* (23), 7391−7399.
(59) Perutz, M. F., Finch, J. T., Berriman, J., and Lesk, A. (2002) Amyloid fibers are water-filled nanotubes. *Proc. Natl. Acad. Sci. U. S. A. 99* (8), 5591−5595.
(60) Singer, S. J., and Dewji, N. N. (2006) Evidence that Perutz's double-beta-stranded subunit structure for beta-amyloidsalso applies to their channel-forming structures in membranes. *Proc. Natl. Acad. Sci. U. S. A. 103*, 1546−1550.
(61) Takahashi, T., Kikuchi, S., Katada, S., Nagai, Y., Nishizawa, M., and Onodera, O. (2008) Soluble polyglutamineoligomers formed prior to inclusion body formation are cytotoxic. *Hum. Mol. Genet. 17*, 345−356.
(62) Chellgren, B. W., Miller, A. F., and Creamer, T. P. (2006) Evidence for polyproline II helical structure in short polyglutamine tracts. *J. Mol. Biol. 361*, 362−371.
(63) Lathrop, R. H., Casale, M., Tobias, D. J., Marsh, J. L., and Thompson, L. M. (1998) Modeling protein homopolymeric repeats: possible polyglutamine structural motifs for Huntington's disease. *Proc. Int. Conf Intell Syst. Mol. Biol. 6*, 105−114.
(64) Armen, R. S., Bernard, B. M., Day, R., Alonso, D. O., and Daggett, V. (2005) Characterization of a possible amyloidogenic precursor in glutamine-repeat neurodegenerative diseases. *Proc. Natl. Acad. Sci. U. S. A. 102*, 13433−13438.
(65) Khare, S. D., Ding, F., Gwanmesia, K. N., and Dokholyan, N. V. (2005) Molecular origin of polyglutamine aggregation in neurodegenerative diseases. *PLoS Comput. Biol. 1*, e30.
(66) Tsukamoto, K., Shimizu, H., Ishida, T., Akiyama, Y., and Nukina, N. (2006) Aggregation mechanism of polyglutamine disease revealed using quantum chemical calculations, fragment molecular orbital calculations, molecular dynamics simulations, and binding free energy calculations. *J. Mol. Struct.: THEOCHEM 778*, 85−95.
(67) Wang, X., Vitalis, A., Wyczalkowski, M. A., and Pappu, R. V. (2006) Characterizing the conformational ensemble of monomeric polyglutamine. *Proteins: Struct., Funct., Genet. 63*, 297−311.
(68) Stork, M., Giese, A., Kretzschmar, H. A., and Tavan, P. (2005) Molecular dynamics simulations indicate a possible role of parallel beta-helices in seeded aggregation of poly-Gln. *Biophys. J. 88*, 2442−2451.
(69) Merlino, A., Esposito, L., and Vitagliano, L. (2006) Polyglutamine repeats and beta-helix structure: Molecular dynamics study. *Proteins: Struct., Funct., Genet. 63* (4), 918−927.
(70) Ogawa, H., Nakano, M., Watanabe, H., Starikov, E. B., Rothstein, S. M., and Tanaka, S. (2008) Molecular dynamics simulation study on the structural stabilities of polyglutamine peptides. *Comput. Biol. Chem. 32* (2), 102−110.
(71) Rossetti, G., Magistrato, A., Pastore, A., Persichetti, F., and Carloni, P. (2008) Structural Properties of Polyglutamine Aggregates Investigated via Molecular Dynamics Simulations. *J. Phys. Chem. B 112* (51), 16843−16850.
(72) Sikorski, P., and Atkins, E. (2005) New model for crystalline polyglutamine assemblies and their connection with amyloid fibrils. *Biomacromolecules 6* (1), 425−432.
(73) Sunde, M., and Blake, C. (1997) The structure of amyloid fibrils by electron microscopy and X-ray diffraction. *Adv. Protein Chem. 50*, 123−159.
(74) Sunde, M., Serpell, L. C., Bartlam, M., Fraser, F. E., Pepys, M. B., and Blake, C. C. F. (1997) Common core structure of amyloid fibrils by synchrotron X-ray diffraction. *J. Mol. Biol. 273* (3), 729−739.
(75) Sharma, D., Shinchuk, L. M., Inouye, H., Wetzel, R., and Kirschner, D. A. (2005) Polyglutamine homopolymers having 8−45 residues form slab-like beta-crystallite assemblies. *Proteins: Struct., Funct., Genet. 61* (2), 398−411.
(76) Finke, J. M., Cheung, M. S., and Onuchic, J. N. (2004) A Structural Model of Polyglutamine Determined from a Host-Guest Method Combining Experiments and Landscape Theory. *Biophys. J. 87* (3), 1900−1918.
(77) Marchut, A. J., and Hall, C. K. (2006) Side-chain interactions determine amyloid formation by model polyglutamine peptides in molecular dynamics simulations. *Biophys. J. 90* (12), 4574−4584.
(78) Marchut, A. J., and Hall, C. K. (2006) Spontaneous formation of annular structures observed in molecular dynamics simulations of polyglutamine peptides. *Comput. Biol. Chem. 30* (3), 215−218.
(79) Marchut, A. J., and Hall, C. K. (2007) Effects of chain length on the aggregation of model polyglutamine peptides: Molecular dynamics simulations. *Proteins: Struct., Funct., Genet. 66* (1), 96−109.
(80) Zanuy, D., Gunasekaran, K., Lesk, A. M., and Nussinov, R. (2006) Computational study of the fibril organization of polyglut-

DOI: 10.1021/acschemneuro.9b00561
ACS Chem. Neurosci. 2020, 11, 105−120

amine repeats reveals a common motif identified in beta-helices. *J. Mol. Biol. 358* (1), 330−345.
(81) Bates, G. (2003) Huntingtin aggregation and toxicity in Huntington's disease. *Lancet 361* (9369), 1642−4.
(82) Ross, C. A., and Poirier, M. A. (2005) What is the role of protein aggregation in neurodegeneration? *Nat. Rev. Mol. Cell Biol. 6* (11), 891−898.
(83) Ross, C. A., Poirier, M. A., Wanker, E. E., and Amzel, M. (2003) Polyglutamine fibrillogenesis: The pathway unfolds. *Proc. Natl. Acad. Sci. U. S. A. 100* (1), 1−3.
(84) Wanker, E. E. (2000) Protein aggregation and pathogenesis of Huntington's disease: mechanisms and correlations. *Biol. Chem. 381* (9−10), 937−942.
(85) Truant, R., Atwal, R. S., Desmond, C., Munsie, L., and Tran, T. (2008) Huntington's disease: revisiting the aggregation hypothesis in polyglutamine neurodegenerative diseases. *FEBS J. 275* (17), 4252−4262.
(86) Zuccato, C., Valenza, M., and Cattaneo, E. (2010) Molecular Mechanisms and Potential Therapeutical Targets in Huntington's Disease. *Physiol. Rev. 90* (3), 905−981.
(87) Lakhani, V. V., Ding, F., and Dokholyan, N. V. (2010) Polyglutamine Induced Misfolding of Huntingtin Exon1 is Modulated by the Flanking Sequences. *PLoS Comput. Biol. 6* (4), No. e1000772.
(88) Kar, K., Jayaraman, M., Sahoo, B., Kodali, R., and Wetzel, R. (2011) Critical nucleus size for disease-related polyglutamine aggregation is repeat-length dependent. *Nat. Struct. Mol. Biol. 18*, 328.
(89) Atwal, R. S., Xia, J., Pinchev, D., Taylor, J., Epand, R. M., and Truant, R. (2007) Huntingtin has a membrane association signal that can modulate huntingtin aggregation, nuclear entry and toxicity. *Hum. Mol. Genet. 16* (21), 2600−15.
(90) Tartari, M., Gissi, C., Lo Sardo, V., Zuccato, C., Picardi, E., Pesole, G., and Cattaneo, E. (2008) Phylogenetic comparison of huntingtin homologues reveals the appearance of a primitive polyQ in sea urchin. *Mol. Biol. Evol. 25* (2), 330−8.
(91) Steffan, J. S., Agrawal, N., Pallos, J., Rockabrand, E., Trotman, L. C., Slepko, N., Illes, K., Lukacsovich, T., Zhu, Y. Z., Cattaneo, E., Pandolfi, P. P., Thompson, L. M., and Marsh, J. L. (2004) SUMO modification of Huntingtin and Huntington's disease pathology. *Science 304* (5667), 100−4.
(92) Klein, F., Pastore, A., Masino, L., Zederlutz, G., Nierengarten, H., Ouladabdelghani, M., Altschuh, D., Mandel, J., and Trottier, Y. (2007) Pathogenic and Non-pathogenic Polyglutamine Tracts Have Similar Structural Properties: Towards a Length-dependent Toxicity Gradient. *J. Mol. Biol. 371* (1), 235−244.
(93) Dehay, B., and Bertolotti, A. (2006) Critical role of the proline-rich region in Huntingtin for aggregation and cytotoxicity in yeast. *J. Biol. Chem. 281* (47), 35608−35615.
(94) Moroni, E., Scarabelli, G., and Colombo, G. (2009) Structure and sequence determinants of aggregation investigated with molecular dynamics. *Front. Biosci., Landmark Ed. 14*, 523−539.
(95) Miller, Y., Ma, B., and Nussinov, R. (2010) Polymorphism in Alzheimer A beta Amyloid Organization Reflects Conformational Selection in a Rugged Energy Landscape. *Chem. Rev. 110* (8), 4820−4838.
(96) Zhou, R. (2003) Trp-cage: Folding Free Energy Landscape in Explicit Water. *Proc. Natl. Acad. Sci. U. S. A. 100*, 13280−13285.
(97) Ma, B., and Nussinov, R. (2006) Simulations as analytical tools to understand protein aggregation and predict amyloid conformation. *Curr. Opin. Chem. Biol. 10* (5), 445−452.
(98) Das, P., King, J. A., and Zhou, R. (2011) Aggregation of gamma-crystallins associated with human cataracts via domain swapping of the C-terminal beta-strands. *Proc. Natl. Acad. Sci. U. S. A. 108*, 10514−10519.
(99) Kelley, N. W., Huang, X., Tam, S., Spiess, C., Frydman, J., and Pande, V. S. (2009) The predicted structure of the headpiece of the huntingtin protein and its implications on huntingtin aggregation. *J. Mol. Biol. 388* (5), 919−927.
(100) Wang, Y., and Voth, G. A. (2010) Molecular Dynamics Simulations of Polyglutamine Aggregation Using Solvent-Free Multiscale Coarse-Grained Models. *J. Phys. Chem. B 114*, 8735.
(101) Papaleo, E., and Invernizzi, G. (2011) Conformational Diseases: Structural Studies of Aggregation of Polyglutamine Proteins. *Curr. Comput.-Aided Drug Des. 7* (1), 23−43.
(102) Zhou, Z., Zhao, J., Liu, H., Wu, J. W., Liu, K., Chuang, C., Tsai, W., and Ho, Y. (2011) The Possible Structural Models for Polyglutamine Aggregation: A Molecular Dynamics Simulations Study. *J. Biomol. Struct. Dyn. 28* (5), 743−758.
(103) Jodeiri Farshbaf, M., and Ghaedi, K. (2017) Huntington's disease and mitochondria. *Neurotoxic. Res. 32*, 518−529.
(104) Arndt, J. R., Chaibva, M., and Legleiter, J. (2015) The emerging role of the first 17 amino acids of huntingtin in Huntington's disease. *Biomol. Concepts 6*, 33−46.
(105) Nakano, M., Ebina, K., and Tanaka, S. (2013) Study of the aggregation mechanism of polyglutamine peptides using replica exchange molecular dynamics simulations. *J. Mol. Model. 19* (4), 1627−1639.
(106) Chen, S. M., Ferrone, F. A., and Wetzel, R. (2002) b Huntington's disease age-of-onset linked to polyglutamine aggregation nucleation. *Proc. Natl. Acad. Sci. U. S. A. 99*, 11884−11889.
(107) Berendsen, H. J. C., van der Spoel, D., and van Drunen, R. (1995) *Comput. Phys. Commun. 91*, 43.
(108) Sugita, Y., and Okamoto, Y. (2000) Replica-exchange multicanonical algorithm and multi-canonical replica-exchange method for simulating systems with rough energy landscape. *Chem. Phys. Lett. 329* (3−4), 261−270.
(109) Dougan, L., Li, J., Badilla, C. L., Berne, B. J., and Fernandez, J. M. (2009) *Proc. Natl. Acad. Sci. U. S. A. 106*, 12605.
(110) Rossetti, G., and Magistrato, A. (2012) Molecular Mechanism of Huntington's Disease — A Computational Perspective, in *Huntington's Disease - Core Concepts and Current Advances* (Tunali, N. E., Ed.), pp 67−98, IntechOpen.
(111) Dickson, C. J., Madej, B. D., Skjevik, Å.A., Betz, R. M., Teigen, K., Gould, I. R., and Walker, R. C. (2014) Lipid14: The Amber Lipid Force Field. *J. Chem. Theory Comput. 10* (2), 865−879.
(112) Gómez-Sicilia, A., Sikora, M., Cieplak, M., and Carrión-Vázquez, M. (2015) An Exploration of the Universe of Polyglutamine Structures. *PLoS Comput. Biol. 11* (10), No. e1004541.
(113) Cossio, P., Trovato, A., Pietrucci, F., Seno, F., Maritan, A., and Laio, A. (2010) Exploring the universe of protein structures beyond the Protein Data Bank. *PLoS Comput. Biol. 6* (11), No. e1000957.
(114) Laghaei, R., and Mousseau, N. (2010) Spontaneous formation of polyglutamine nanotubes with molecular dynamics simulations. *J. Chem. Phys. 132* (16), 165102.
(115) Miettinen, M. S., Knecht, V., Monticelli, L., and Ignatova, Z. (2012) Assessing polyglutamine conformation in the nucleating event by molecular dynamics simulations. *J. Phys. Chem. B 116* (34), 10259−10265.
(116) Kaminski, G. A., Friesner, R. A., Tirado-Rives, J., and Jorgensen, W. L. (2001) *J. Phys. Chem. B 105*, 6474.
(117) Zhang, Q. C., Yeh, T. L., Leyva, A., Frank, L. G., Miller, J., Kim, Y. E., Langen, R., Finkbeiner, S., Amzel, M. L., Ross, C. A., and Poirier, M. A. (2011) A Compact beta Model of huntingtin Toxicity. *J. Biol. Chem. 286* (10), 8188−8196.
(118) Tozzini, V. (2010) Multiscale Modeling of Proteins. *Acc. Chem. Res. 43* (2), 220−230.
(119) Rossetti, G., Magistrato, A., Pastore, A., and Carloni, P. (2010) Hydrogen Bonding Cooperativity in polyQ beta-Sheets from First Principle Calculations. *J. Chem. Theory Comput. 6* (6), 1777−1782.
(120) Carloni, P., Rothlisberger, U., and Parrinello, M. (2002) The Role and Perspective of Ab Initio Molecular Dynamics in the Study of Biological Systems. *Acc. Chem. Res. 35* (6), 455−464.
(121) Laio, A., and Gervasio, F. L. (2008) Metadynamics: a method to simulate rare events and reconstruct the free energy in biophysics, chemistry and material science. *Rep. Prog. Phys. 71* (12), 126601.

DOI: 10.1021/acschemneuro.9b00561
ACS Chem. Neurosci. 2020, 11, 105−120

(122) Christ, C. D., Mark, A. E., and van Gunsteren, W. F. (2009) Basic ingredients of free energy calculations: A review. *J. Comput. Chem. 31* (8), 1569−1582.
(123) Biarnes, X., Bongarzone, S., Vargiu, A., Carloni, P., and Ruggerone, P. (2011) Molecular motions in drug design: the coming age of the meta-dynamics method. *J. Comput.-Aided Mol. Des. 25* (5), 395−402.
(124) Bussi, G., Gervasio, F. L., Laio, A., and Parrinello, M. (2006) Free-Energy Landscape for Œ≤ Hairpin Folding from Combined Parallel Tempering and Metadynamics. *J. Am. Chem. Soc. 128* (41), 13435−13441.
(125) Horvath, V., Varga, Z., and Kovacs, A. (2004) Long-range effects in oligopeptides. A theoretical study of the beta-sheet structure of Gly(n) (n = 2−10). *J. Phys. Chem. A 108* (33), 6869−6873.
(126) Horvath, V., Varga, Z., and Kovacs, A. (2005) Substituent effects on long-range interactions in the β-sheet structure of oligopeptides. *J. Mol. Struct.: THEOCHEM 755* (1−3), 247−251.
(127) Barton, S., Jacak, R., Khare, S. D., Ding, F., and Dokholyan, N. V. (2007) The length dependence of the polyQ-mediated protein aggregation. *J. Biol. Chem. 282* (35), 25487−92.
(128) Angeli, S., Shao, J., and Diamond, M. I. (2010) F-actin binding regions on the androgen receptor and huntingtin increase aggregation and alter aggregate characteristics. *PLoS One 5* (2), No. e9053.
(129) Wanker, E. E., Scherzinger, E., Heiser, V., Sittler, A., Eickhoff, H., and Lehrach, H. (1999) Membrane filter assay for detection of amyloid-like polyglutamine-containing protein aggregates. *Methods Enzymol. 309*, 375−386.
(130) Rambaran, R. N., and Serpell, L. C. (2008) Amyloid fibrils Abnormal protein assembly. *Prion 2*, 112−117.
(131) Saunders, H. M., Hughes, V. A., Cappai, R., and Bottomley, S. P. (2013) Conformational Behavior and Aggregation of Ataxin-3 in SDS. *PLoS One 8*, No. e69416.
(132) Masino, L., Nicastro, G., Menon, R. P., Piaz, F. D., Calder, L., and Pastore, A. (2004) Characterization of the structure and the amyloidogenic properties of the Josephin domain of the polyglutamine-containing protein ataxin-3. *J. Mol. Biol. 344*, 1021−1035.
(133) Legleiter, J., Mitchell, E., Lotz, G. P., Sapp, E., Ng, C., DiFiglia, M., Thompson, L. M., and Muchowski, P. J. (2010) Mutant Huntingtin Fragments Form Oligomers in a Polyglutamine Length-dependent Manner in Vitro and in Vivo. *J. Biol. Chem. 285*, 14777−14790.
(134) Bhattacharyya, A. M., Thakur, A. K., and Wetzel, R. (2005) Polyglutamine aggregation nucleation: Thermodynamics of a highly unfavorable protein folding reaction. *Proc. Natl. Acad. Sci. U. S. A. 102*, 15400−15405.
(135) Thakur, A. K., and Wetzel, R. (2002) Mutational analysis of the structural organization of polyglutamine aggregates. *Proc. Natl. Acad. Sci. U. S. A. 99*, 17014−17019.
(136) Goldsbury, C. S., Cooper, G. J. S., Goldie, K. N., Muller, S. A., Saafi, E. L., Gruijters, W. T. M., Misur, M. P., et al. (1997) Polymorphic fibrillar assembly of human amylin. *J. Struct. Biol. 119*, 17−27.
(137) Scherzinger, E., Lurz, R., Turmaine, M., Mangiarini, L., Hollenbach, B., Hasenbank, R., Bates, G. P., Davies, S. W., Lehrach, H., and Wanker, E. E. (1997) Huntingtin-encoded polyglutamine expansions form amyloid-like protein aggregates in vitro and in vivo. *Cell 90*, 549−558.
(138) Poirier, M. A., Li, H. L., Macosko, J., Cai, S. W., Amzel, M., and Ross, C. A. (2002) Huntingtin spheroids and protofibrils as precursors in polyglutamine fibrilization. *J. Biol. Chem. 277*, 41032−41037.
(139) Sivanandam, V. N., Jayaraman, M., Hoop, C. L., Kodali, R., Wetzel, R., and van der Wel, P. C. A. (2011) The Aggregation-Enhancing Huntingtin N-Terminus Is Helical in Amyloid Fibrils. *J. Am. Chem. Soc. 133*, 4558−4566.
(140) Yates, E. A., Cucco, E. M., and Legleiter, J. (2011) Point Mutations in Aβ Induce Polymorphic Aggregates at Liquid/Solid Interfaces. *ACS Chem. Neurosci. 2*, 294−307.
(141) Bugg, C. W., Isas, J. M., Fischer, T., Patterson, P. H., and Langen, R. (2012) Structural features and domain organization of huntingtin fibrils. *J. Biol. Chem. 287* (38), 31739.
(142) Mishra, R., Hoop, C. L., Kodali, R., Sahoo, B., van der Wel, P. C. A., and Wetzel, R. (2012) Serine Phosphorylation Suppresses Huntingtin Amyloid Accumulation by Altering Protein Aggregation Properties. *J. Mol. Biol. 424*, 1−14.
(143) Hoop, C. L., Lin, H. K., Kar, K., Magyarfalvi, G., Lamley, J. M., Boatz, J. C., Mandal, A., Lewandowski, J. R., Wetzel, R., and van der Wel, P. C. A. (2016) Huntingtin exon 1 fibrils feature an interdigitated beta-hairpin-based polyglutamine core. *Proc. Natl. Acad. Sci. U. S. A. 113*, 1546−1551.
(144) Duennwald, M. L., Jagadish, S., Muchowski, P. J., and Lindquist, S. (2006) Flanking sequences profoundly alter polyglutamine toxicity in yeast. *Proc. Natl. Acad. Sci. U. S. A. 103*, 11045−11050.
(145) Robertson, A. L., Horne, J., Ellisdon, A. M., Thomas, B., Scanlon, M. J., and Bottomley, S. P. (2008) The Structural Impact of a Polyglutamine Tract Is Location-Dependent. *Biophys. J. 95*, 5922−5930.
(146) Saunders, H. M., and Bottomley, S. P. (2009) Multi-domain misfolding: understanding the aggregation pathway of polyglutamine proteins. *Protein Eng., Des. Sel. 22*, 447−451.
(147) Saunders, H. M., Gilis, D., Rooman, M., Dehouck, Y., Robertson, A. L., and Bottomley, S. P. (2011) Flanking domain stability modulates the aggregation kinetics of a polyglutamine disease protein. *Protein Sci. 20*, 1675−1681.
(148) Burke, K. A., Kauffman, K. J., Umbaugh, C. S., Frey, S. L., and Legleiter, J. (2013) The Interaction of Polyglutamine Peptides with Lipid Membranes Is Regulated by Flanking Sequences Associated with Huntingtin. *J. Biol. Chem. 288*, 14993−15005.
(149) Eftekharzadeh, B., Piai, A., Chiesa, G., Mungianu, D., Garcia, J., Pierattelli, R., Felli, I. C., and Salvatella, X. (2016) Sequence Context Influences the Structure and Aggregation Behavior of a PolyQ Tract. *Biophys. J. 110*, 2361−2366.
(150) Darnell, G. D., Derryberry, J., Kurutz, J. W., and Meredith, S. C. (2009) Mechanism of Cis-Inhibition of PolyQ Fibrillation by PolyP: PPII Oligomers and the Hydrophobic Effect. *Biophys. J. 97*, 2295−2305.
(151) Williamson, T. E., Vitalis, A., Crick, S. L., and Pappu, R. V. (2010) Modulation of Polyglutamine Conformations and Dimer Formation by the N-Terminus of Huntingtin. *J. Mol. Biol. 396*, 1295−1309.
(152) Burke, K. A., Godbey, J., and Legleiter, J. (2011) Assessing mutant huntingtin fragment and polyglutamine aggregation by atomic force microscopy. *Methods 53*, 275−284.
(153) Monsellier, E., Redeker, V., Ruiz-Arlandis, G., Bousset, L., and Melki, R. (2015) Molecular Interaction between the Chaperone Hsc70 and the N-terminal Flank of Huntingtin Exon 1 Modulates Aggregation. *J. Biol. Chem. 290*, 2560−2576.
(154) Michalek, M., Salnikov, E. S., Werten, S., and Bechinger, B. (2013) a Membrane Interactions of the Amphipathic Amino Terminus of Huntingtin. *Biochemistry 52*, 847−858.
(155) Côté, S., Binette, V., Salnikov, E. S., Bechinger, B., and Mousseau, N. (2015) Probing the Huntingtin 1−17 Membrane Anchor on a Phospholipid Bilayer by Using All-Atom Simulations. *Biophys. J. 108*, 1187−1198.
(156) Chaibva, M., Burke, K. A., and Legleiter, J. (2014) Curvature Enhances Binding and Aggregation of Huntingtin at Lipid Membranes. *Biochemistry 53*, 2355−2365.
(157) Nagarajan, A., Jawahery, S., and Matysiak, S. (2014) The effects of flanking sequences in the interaction of polyglutamine peptides with a membrane bilayer. *J. Phys. Chem. B 118*, 6368−6379.
(158) Levy, G. R., Shen, K., Gavrilov, Y., Smith, P. E. S., Levy, Y., Chan, R., Frydman, J., and Frydman, L. (2019) Huntingtin's N-Terminus Rearrangements in the Presence of Membranes: A Joint Spectroscopic and Computational Perspective. *ACS Chem. Neurosci. 10*, 472−481.

DOI: 10.1021/acschemneuro.9b00561
ACS Chem. Neurosci. 2020, 11, 105−120

(159) Straub, J. E., and Thirumalai, D. (2011) Toward a molecular theory of early and late events in monomer to amyloid fibril formation. *Annu. Rev. Phys. Chem. 62*, 437−463.
(160) Rojas, A. V., Liwo, A., and Scheraga, H. A. (2011) A Study of the alpha-Helical Intermediate Preceding the Aggregation of the Amino-Terminal Fragment of the beta Amyloid Peptide. *J. Phys. Chem. B 115*, 12978−12983.
(161) Lyubchenko, Y. L., et al. (2012) Fibrillogenesis of Huntingtin and Other Glutamine Containing Proteins. *Subcell. Biochem. 65*, 225−251.
(162) Palazzolo, I., Burnett, B. G., Young, J. E., Brenne, P. L., La Spada, A. R., Fischbeck, K. H., Howell, B. W., and Pennuto, M. (2007) Akt blocks ligand binding and protects against expanded polyglutamine androgen receptor toxicity. *Hum. Mol. Genet. 16*, 1593−1603.
(163) Mukherjee, S., Thomas, M., Dadgar, N., Lieberman, A. P., and Iniguez-Lluhi, J. A. (2009) Small Ubiquitin-like Modifier (SUMO) Modification of the Androgen Receptor Attenuates Polyglutamine-mediated Aggregation. *J. Biol. Chem. 284*, 21296−21306.
(164) Watkin, E. E., Arbez, N., Waldron-Roby, E., O'Meally, R., Ratovitski, T., Cole, R. N., and Ross, C. A. (2014) Phosphorylation of Mutant Huntingtin at Serine 116 Modulates Neuronal Toxicity. *PLoS One 9*, No. e88284.
(165) Aiken, C. T., Steffan, J. S., Guerrero, C. M., Khashwji, H., Lukacsovich, T., Simmons, D., Purcell, J. M., Menhaji, K., Zhu, Y. Z., Green, K., LaFerla, F., Huang, L., Thompson, L. M., and Marsh, J. L. (2009) Phosphorylation of Threonine 3. Implications for Huntingtin Aggregation and Neurotoxicity. *J. Biol. Chem. 284*, 29427−29436.
(166) Thompson, L. M., Aiken, C. T., Kaltenbach, L. S., Agrawal, N., Illes, K., Khoshnan, A., Martinez-Vincente, M., Arrasate, M., O'Rourke, J. G., Khashwji, H., Lukacsovich, T., Zhu, Y. Z., Lau, A. L., Massey, A., Hayden, M. R., Zeitlin, S. O., Finkbeiner, S., Green, K. N., LaFerla, F. M., Bates, G., Huang, L., Patterson, P. H., Lo, D. C., Cuervo, A. M., Marsh, J. L., and Steffan, J. S. (2009) IKK phosphorylates Huntingtin and targets it for degradation by the proteasome and lysosome. *J. Cell Biol. 187*, 1083−1099.
(167) Gu, X., Greiner, E. R., Mishra, R., Kodali, R., Osmand, A., Finkbeiner, S., Steffan, J. S., Thompson, L. M., Wetzel, R., and Yang, X. W. (2009) Serines 13 and 16 Are Critical Determinants of Full-Length Human Mutant Huntingtin Induced Disease Pathogenesis in HD Mice. *Neuron 64*, 828−840.
(168) Ehrnhoefer, D. E., Sutton, L., and Hayden, M. R. (2011) Small Changes, Big Impact: Posttranslational Modifications and Function of Huntingtin in Huntington Disease. *Neuroscientist 17*, 475−492.
(169) Warby, S. C., Doty, C. N., Graham, R. K., Carroll, J. B., Yang, Y. Z., Singaraja, R. R., Overall, C. M., and Hayden, M. R. (2008) Activated caspase-6 and caspase-6-cleaved fragments of huntingtin specifically colocalize in the nucleus. *Hum. Mol. Genet. 17*, 2390−2404.
(170) Humbert, S., and Saudou, F. (2003) Huntingtin phosphorylation and signaling pathways that regulate toxicity in Huntington's disease. *Clin. Neurosci. Res. 3*, 149−155.
(171) Chaibva, M., Jawahery, S., Pilkington, A. W. T., Arndt, J. R., Sarver, O., Valentine, S., Matysiak, S., and Legleiter, J. (2016) Acetylation within the First 17 Residues of Huntingtin Exon 1 Alters Aggregation and Lipid Binding. *Biophys. J. 111*, 349−362.
(172) Gorbenko, G. P., and Kinnunen, P. K. J. (2006) The role of lipid-protein interactions in amyloid-type protein fibril formation. *Chem. Phys. Lipids 141*, 72−82.
(173) Burke, K. A., Yates, E. A., and Legleiter, J. (2013) a Biophysical insights into how surfaces, including lipid membranes, modulate protein aggregation related to neurodegeneration. *Front Neurol. 4*, 17.
(174) Kegel-Gleason, K. B. (2013) Huntingtin Interactions with Membrane Phospholipids: Strategic Targets for Therapeutic Intervention? *J. Huntington's Dis. 2*, 239−250.
(175) Kegel, K. B., Sapp, E., Alexander, J., Valencia, A., Reeves, P., Li, X., Masso, N., Sobin, L., Aronin, N., and DiFiglia, M. (2009) Polyglutamine expansion in huntingtin alters its interaction with phospholipids. *J. Neurochem. 110*, 1585−1597.
(176) Cattaneo, E., Rigamonti, D., Goffredo, D., Zuccato, C., Squitieri, F., and Sipione, S. (2001) Loss of normal huntingtin function: new developments in Huntington's disease research. *Trends Neurosci. 24* (3), 182−188.
(177) Slepnev, V. I., and De Camilli, P. (2000) Accessory factors in clathrin-dependent, synaptic vesicle endocytosis. *Nat. Rev. Neurosci. 1*, 161−172.
(178) Sun, Y., Savanenin, A., Reddy, P. H., and Liu, Y. F. (2001) Polyglutamine-expanded huntingtin promotes sensitization of N-methyl-D-aspartate receptors via post-synaptic density. *J. Biol. Chem. 276*, 24713−24718.
(179) Gopalakrishnan, C., Kalsi, N., Jethi, S., and Purohit, R. (2015) Computational investigation of molecular mechanism and neuro-pathological implications in Huntington disease. *Mol. Cell. Biochem. 409*, 1−11.
(180) Gao, Y.-G., Yan, X.-Z., Song, A.-X., Chang, Y.-G., Gao, X.-C., Jiang, N., Zhang, Q., and Hu, H.-Y. (2006) Structural insights into the specific binding of Huntingtin proline-rich region with the SH3 and WW domains. *Structure 14* (12), 1755−1765.
(181) Sittler, A., Walter, S., Wedemeyer, N., Hasenbank, R., Scherzinger, E., Eickhoff, H., Bates, G. P., Lehrach, H., and Wanker, E. E. (1998) SH3GL3 associates with the huntingtin exon 1protein and promotes the formation of polygln-containing protein aggregates. *Mol. Cell 2*, 427−436.
(182) Vöpel, T., Bravo-Rodriguez, K., Mittal, S., Vachharajani, S., Gnutt, D., Sharma, A., Steinhof, A., Fatoba, O., Ellrichmann, G., Nshanian, M., Heid, C., Loo, J. A., Klärner, F.-G., Schrader, T., Bitan, G., Wanker, E. E., Ebbinghaus, S., and Sanchez-Garcia, E. (2017) Inhibition of Huntingtin exon-1 aggregation by the molecular tweezer CLR01. *J. Am. Chem. Soc. 139* (16), 5640−5643.
(183) Sinha, S., Lopes, D. H., Du, Z., Pang, E. S., Shanmugam, A., Lomakin, A., Talbiersky, P., Tennstaedt, A., McDaniel, K., Bakshi, R., Kuo, P. Y., Ehrmann, M., Benedek, G. B., Loo, J. A., Klärner, F. G., Schrader, T., Wang, C., and Bitan, G. (2011) *J. Am. Chem. Soc. 133*, 16958.
(184) Talbiersky, P., Bastkowski, F., Klärner, F. G., and Schrader, T. (2008) *J. Am. Chem. Soc. 130*, 9824.
(185) Caterino, M., Squillaro, T., Montesarchio, D., Giordano, A., Giancola, C., and Melone, M. A. B. (2018) Huntingtin protein: A new option for fixing the Huntington's disease countdown clock. Review article. *Neuropharmacology 135*, 126−138.
(186) Gagnon, K. T., Pendergraff, H. M., Deleavey, G. F., Swayze, E. E., Potier, P., Randolph, J., Roesch, E. B., Chattopadhyaya, J., Damha, M. J., Bennett, C. F., Montaillier, C., Lemaitre, M., and Corey, D. R. (2010) Allele-selective inhibition of mutant huntingtin expression with antisense oligonucleotides targeting the expanded CAG repeat. *Biochemistry 49*, 10166−10178.
(187) Ostergaard, M. E., Southwell, A. L., Kordasiewicz, H., Watt, A. T., Skotte, N. H., Doty, C. N., Vaid, K., Villanueva, E. B., Swayze, E. E., Bennett, C. F., Hayden, M. R., and Seth, P. P. (2013) Rational design of antisense oligonucleotides targeting single nucleotide polymorphisms for potent and allele selective suppression of mutant Huntingtin in the CNS. *Nucleic Acids Res. 41*, 9634−9650.
(188) Ostergaard, M. E., Kumar, P., Nichols, J., Watt, A., Sharma, P. K., Nielsen, P., and Seth, P. P. (2015) Allele-selective inhibition of mutant huntingtin with 2-thio- and C5- Triazolylphenyl-Deoxythymidine-Modified antisense oligonucleotides. *Nucleic Acid Ther. 25*, 266−274.
(189) Zaghloul, E. M., Gissberg, O., Moreno, P. M. D., Siggens, L., Hallbrink, M., Jorgensen, A. S., Ekwall, K., Zain, R., Wengel, J., Lundin, K. E., and Smith, C. I. E. (2017) CTG repeat-targeting oligonucleotides for down-regulating Huntingtin expression. *Nucleic Acids Res. 45*, 5153−5169.
(190) Sridharan, K., and Gogtay, N. J. (2016) Therapeutic nucleic acids: current clinical status. *Br. J. Clin. Pharmacol. 82*, 659−672.
(191) Wolter, O., and Mayer, G. (2017) Aptamers as valuable molecular tools in neurosciences. *J. Neurosci. 37*, 2517−2523.

DOI: 10.1021/acschemneuro.9b00561
ACS Chem. Neurosci. 2020, 11, 105−120

(192) Aguiar, S., van der Gaag, B., and Cortese, F. A. B. (2017) RNAi mechanisms in Huntington's disease therapy: siRNA versus shRNA. *Transl. Neurodegener. 6*, 30.
(193) Case, D. A., Cheatham, T. E., III, Darden, T., Gohlke, H., Luo, R., Merz, K. M., Jr., Onufriev, A., Simmerling, C., Wang, B., and Woods, R. J. (2005) *J. Comput. Chem. 26*, 1668−1688.
(194) Duan, Y., Wu, C., Chowdhury, S., Lee, M. C., Xiong, G., Zhang, W., Yang, R., Cieplak, P., Luo, R., Lee, T., Caldwell, J., Wang, J., and Kollman, P. J. (2003) *J. Comput. Chem. 24*, 1999−2012.
(195) Mathias, G., Egwolf, B., Nonella, M., and Tavan, P. (2003) A fast multi-pole method combined with a reaction field for long-range electrostatics in molecular dynamics simulations: The effects of truncation on the properties of water. *J. Chem. Phys. 118*, 10847−10860.
(196) Lyubartsev, A. P., Martsinovski, A. A., Shevkunov, S. V., and Vorontsov-Velyaminov, P. N. (1992) New approach to Monte Carlo calculation of the free energy: Method of expanded ensembles. *J. Chem. Phys. 96*, 1776−1783.

DOI: 10.1021/acschemneuro.9b00561
ACS Chem. Neurosci. 2020, 11, 105−120